

Articles

Evolution of a Highly Selective and Potent 2-(Pyridin-2-yl)-1,3,5-triazine Tie-2 Kinase Inhibitor

Brian L. Hodous,^{*,†} Stephanie D. Geuns-Meyer,[†] Paul E. Hughes,[‡] Brian K. Albrecht,[†] Steve Bellon,[§] James Bready,[‡] Sean Caenepeel,[‡] Victor J. Cee,[†] Stuart C. Chaffee,[†] Angela Coxon,[‡] Maurice Emery,^{||} Jenne Fretland,^{||} Paul Gallant,[⊥] Yan Gu,[⊥] Doug Hoffman,[∞] Rebecca E. Johnson,[†] Richard Kendall,[‡] Joseph L. Kim,[§] Alexander M. Long,[§] Michael Morrison,[⊥] Philip R. Olivieri,[†] Vinod F. Patel,[†] Anthony Polverino,[‡] Paul Rose,[⊥] Paul Tempest,[†] Ling Wang,[‡] Douglas A. Whittington,[§] and Huilin Zhao[⊥]

Departments of Medicinal Chemistry, Molecular Pharmacology, and Molecular Structure, Amgen Inc., One Kendall Square, Building 1000, Cambridge, Massachusetts 02139-1581, and Departments of Oncology Research, Pharmaceuticals, and Pharmacokinetics and Drug Metabolism, Amgen Inc., One Amgen Center Drive, Thousand Oaks, California 91320-1799

Received September 22, 2006

Inhibition of angiogenesis is a promising and clinically validated approach for limiting tumor growth and survival. The receptor tyrosine kinase Tie-2 is expressed almost exclusively in the vascular endothelium and is required for developmental angiogenesis and vessel maturation. However, the significance of Tie-2 signaling in tumor angiogenesis is not well understood. In order to evaluate the therapeutic utility of inhibiting Tie-2 signaling, we developed a series of potent and orally bioavailable small molecule Tie-2 kinase inhibitors with selectivity over other kinases, especially those that are believed to be important for tumor angiogenesis. Our earlier work provided pyridinyl pyrimidine **6** as a potent, nonselective Tie-2 inhibitor that was designed on the basis of X-ray cocrystal structures of KDR inhibitors **34** (triazine) and **35** (nicotinamide). Lead optimization resulted in pyridinyl triazine **63**, which exhibited >30-fold selectivity over a panel of kinases, good oral exposure, and in vivo inhibition of Tie-2 phosphorylation.

Introduction

Angiogenesis,¹ the formation of new capillaries from preexisting blood vessels, is implicated in major diseases such as rheumatoid arthritis,² psoriasis,³ and cancer.⁴ In the oncology setting, angiogenesis is believed to be necessary for solid tumors to grow beyond a diameter of about 1–2 mm, the size at which diffusion may no longer suffice to supply oxygen and nutrients and remove waste.^{4,5}

Receptor tyrosine kinases (RTK) represent a large family of membrane-bound enzymes responsible for a diverse range of biological processes, including relay of angiogenic signals from tumor-secreted growth factors.⁶ These proteins all consist of an extracellular ligand-binding domain, a transmembrane region, and an intracellular kinase domain (ATP binding).

RTKs known to be involved in tumor angiogenesis are the vascular endothelial growth factor receptor (VEGFR) tyrosine kinase family members.⁷ In particular, KDR (VEGFR-2) has been shown to play essential roles in endothelial cell migration and proliferation, two critical steps in angiogenesis. A large number of ATP-competitive small molecule KDR inhibitors^{8,9} have been reported in the literature, and several have advanced into late-stage clinical trials and been approved by the FDA, including **1** (PTK787/vatalanib),¹⁰ **2** (SU-11248/sunitinib/Sutent),¹¹ and **3** (BAY 43–9006/sorafenib/Nexavar)¹² (Figure

1). A humanized monoclonal antibody that prevents VEGF from binding to its receptor, bevacizumab (Avastin),¹³ was approved by the FDA in 2003 for first-line treatment of metastatic colorectal cancer.

Whereas VEGF and KDR are well-validated tumor angiogenesis targets, a less well understood area of study in angiogenesis involves the competing interactions of angiopoietins (Ang-1 and Ang-2) with the Tie-2 receptor (tyrosine kinase with immunoglobulin and epidermal growth factor homology domains-2).¹⁴ Tie-2 is an endothelial cell specific receptor tyrosine kinase that is involved in angiogenic processes such as vessel branching, sprouting, remodeling, maturation, and stability.¹⁴ Angiopoietin-1 binds to Tie-2 and stimulates tyrosine phosphorylation and signal transduction.¹⁵ This agonist/receptor interaction stabilizes blood vessels by recruiting perivascular cells and enhances interactions between endothelial cells and vascular smooth muscle cells. The result is blood vessel formation and/or maintenance, depending most likely on the aggregation state of Tie-2 and relative level of supportive growth factor expression.^{14a} It has been shown that Ang-1 interaction with Tie-2 can enhance VEGF/KDR-induced angiogenesis, suggesting there is a cooperative effect of these growth factors. Ang-2 competes with Ang-1 for Tie-2 receptor binding. Several studies suggest that Ang-2 can play the role of agonist or antagonist of Tie-2 signaling depending on the context.^{14,16} Ang-2 binds to Tie-2 and destabilizes vasculature, which initiates angiogenesis in the presence of VEGF and other proangiogenic factors, but may lead to vessel regression in the absence of these collaborative growth factors.

In order to assess the usefulness of direct inhibition of Tie-2 signaling as a cancer therapy (alone or in conjunction with inhibition of other angiogenic kinases), it would be desirable

* To whom correspondence should be addressed. Tel: 617-444-5090. Fax: 617-621-3908. E-mail: bhodous@amgen.com.

[†] Department of Medicinal Chemistry.

[‡] Department of Oncology Research.

[§] Department of Molecular Structure.

^{||} Department of Pharmacokinetics and Drug Metabolism.

[⊥] Department of Molecular Pharmacology.

[∞] Department of Pharmaceuticals.

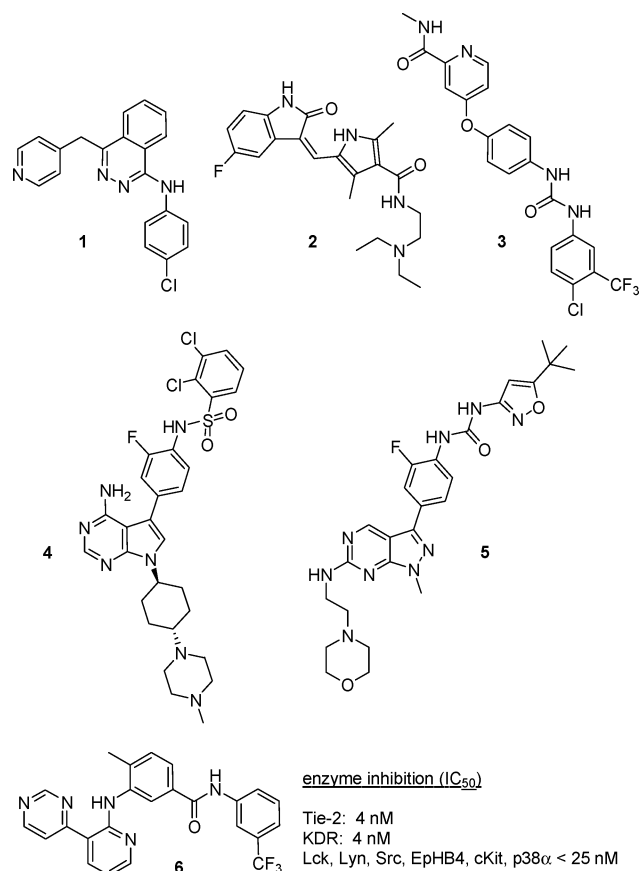


Figure 1. Previously reported KDR (1-3) and Tie-2 (4, 5) inhibitors, and a potent, multi-kinase inhibitor (6).

to have a selective small molecule Tie-2 inhibitor that is free of confounding activities against other kinases that play a role in tumor angiogenesis. In contrast to the plethora of small molecule inhibitors of KDR in the literature,⁸ to the best of our knowledge, there are only two reports of small molecule Tie-2 inhibitors that are highly selective over KDR (Figure 1).¹⁷ The first reported example is **4**, described by Abbott Laboratories in 2001 as a potent inhibitor of Tie-2 (> 100-fold selective over KDR), possessing antiangiogenic properties *in vivo*.^{17a,b} In 2005, GlaxoSmithKline reported **5** as a selective Tie-2 inhibitor (> 140-fold selective over KDR) that also demonstrated potency in a matrigel model of angiogenesis.^{17c}

In this paper, we disclose the design and optimization of a novel class of potent and selective pyridinyl pyrimidine and pyridinyl triazine Tie-2 inhibitors.¹⁸ Potent multi-kinase inhibitor **6** (Figure 1) was designed on the basis of overlay of X-ray cocrystal structures of two different KDR inhibitor scaffolds (inhibitors **34** and **35**, Figure 2). As a result of the modularity of the resulting hybrid structure (**36** → **6**), the nature of the chemical groups attached to the pyridine core was diversified in a relatively small number of straightforward chemical steps. Selectivity over other kinases known to be involved in angiogenesis, especially KDR, was achieved and will be crucial for interpretation of *in vivo* disease model-based experiments.

Chemistry

The general structures of interest **A** were synthesized starting from multifunctional pyridine derivatives **D** (Scheme 1).¹⁸ A variety of chemical approaches were implemented to construct **D**, ranging from classical heterocyclic chemistry to construct pyrimidine and triazine rings to modern Suzuki cross-coupling reactions utilizing heteroaryl halides and pyridine boronic acids.

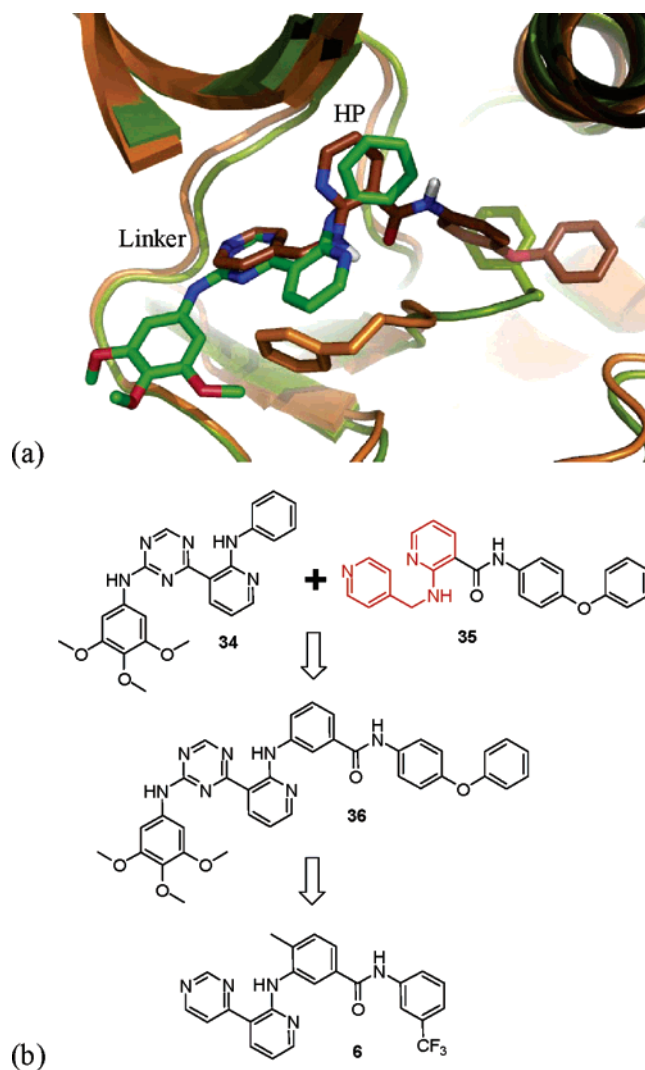


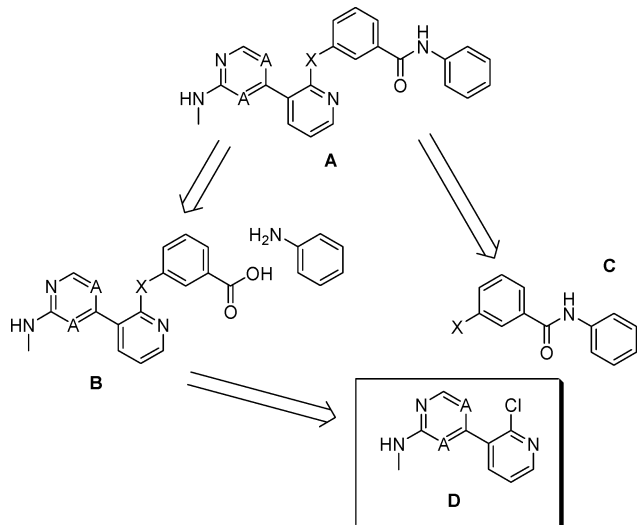
Figure 2. (a) X-ray cocrystal structures of triazine **34** (green; DFG-in conformation) and nicotinamide **35** (brown; DFG-out conformation) bound to the ATP binding site of KDR. Good superimposition of the two linker-binding rings and aromatic moieties in the hydrophobic pocket (HP) was observed (oxygen atoms = red, nitrogen atoms = blue). (b) Emergence of a novel DFG-out binding scaffold (**36** reduced to **6**) based on interpretation of X-ray cocrystal structure data.

Incorporation of diversity into the right-hand side of the molecule was accomplished via one of two direct routes highlighted in detail in the following schemes. Penultimate intermediates **B–D** were accessible on multigram scale to expedite broad structure–activity relationship (SAR) studies within this structural class.

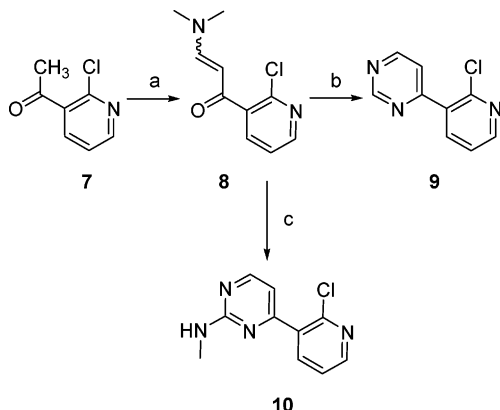
Pyrimidine cores **9** and **10** were synthesized via a two-step sequence from known methyl ketone **7** (which was synthesized from readily available 2-chloronicotiny chloride) (Scheme 2).¹⁹ Dimethylformamide dimethylacetal reacted with **7** to provide enaminone **8** in 56% yield as a light yellow solid. Condensation of **8** with either formamidine or *N*-methylguanidine yielded 2-chloropyridine derivatives **9** and **10**, respectively, in 80–90% yield. These intermediates were subsequently reacted with an aminobenzoic acid (such as **11**) under mixed acid/base conditions ($\text{Et}_3\text{N}\cdot\text{TFA}$) to produce biaryl aniline penultimate intermediate **12** in 71% yield via nucleophilic aromatic substitution of the activated chloride (Scheme 3).

Corresponding ether derivatives **15** were similarly formed from hydroxybenzoic acids, such as **13**, and an inorganic base to generate biaryl ether **14** in 87% yield (Scheme 4). The benzoic

Scheme 1. Retrosynthesis of Pyridinyl Heterocycles

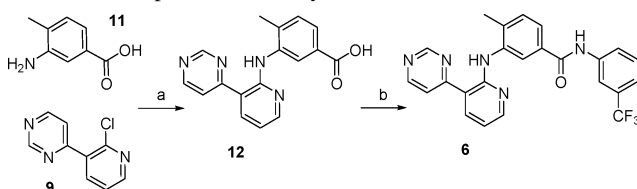


Scheme 2. Preparation of Pyridinyl Pyrimidines^a



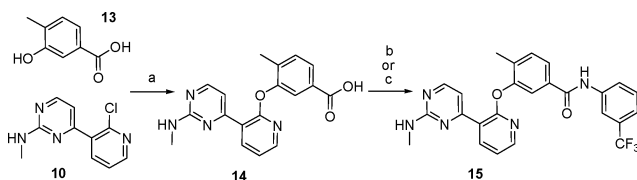
^a Reagents and conditions: (a) dimethylformamide dimethylacetal, 85 °C; (b) formamidine·HCl, Na⁰, MeOH, 55 °C; (c) *N*-methylguanidine·HCl, Na⁰, MeOH, 55 °C.

Scheme 3. Preparation of Biaryl Anilines^a



^a Reagents and conditions: (a) Et₃N·TFA, DMSO, 95 °C; (b) 3-trifluoromethylaniline, EDC, DMAP, DMF, 65 °C.

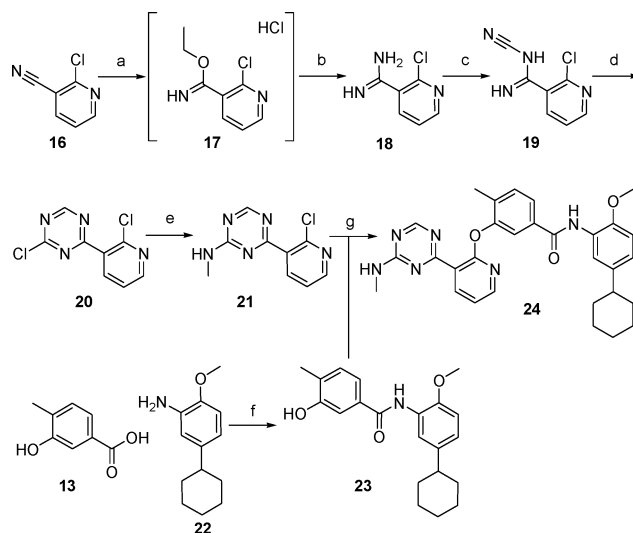
Scheme 4. Preparation of Biaryl Ethers^a



^a Reagents and conditions: (a) Cs₂CO₃, DMSO, 130 °C; (b) 3-trifluoromethylphenyl acyl chloride, HATU, Et₃N, CHCl₃, 65 °C; (c) (i) oxalyl chloride, DMF, THF, rt, (ii) 3-trifluoromethylphenyl acyl chloride, THF, rt–65 °C.

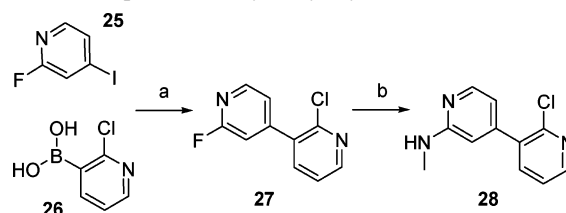
acid intermediates **14** (Scheme 4) and **12** (Scheme 3) were converted to amides (**15** and **6**, respectively) by EDC- or HATU-mediated reactions or through the acyl chloride intermediate. Target molecules **6**, **15**, **37–48**, and **52–58** (Tables 1–4) were provided via these general synthetic methods.

Scheme 5. Preparation of Pyridinyl Triazines and an Alternative Synthetic Route to Analogs^a



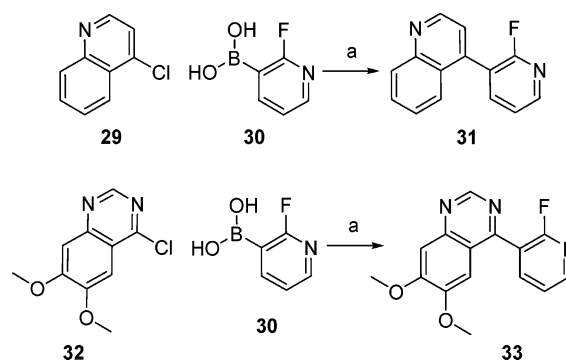
^a Reagents and conditions: (a) HCl, EtOH, 0 °C; (b) NH₄OAc, *i*-PrOH, rt; (c) H₂CN₂, NaHCO₃, *i*-PrOH, H₂O, rt; (d) POCl₃, DMF, CH₃CN, CH₂Cl₂, rt; (e) MeNH₂, CH₂Cl₂, rt; (f) PCl₃, DMAP, toluene, reflux, Dean–Stark apparatus; (g) Cs₂CO₃, DMSO, 130 °C.

Scheme 6. Preparation of Pyridinyl Pyridines^a



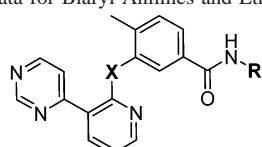
^a Reagents and conditions: (a) Pd(OAc)₂, *t*-Bu₃P·HBF₄, Na₂CO₃, dioxane, H₂O, 100 °C; (b) MeNH₂, THF, 80 °C.

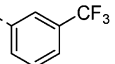
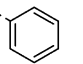
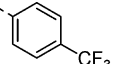
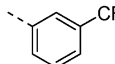
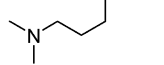
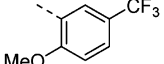
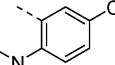
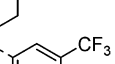
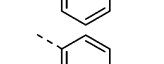
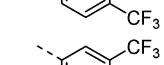
Scheme 7. Preparation of Pyridinyl Quinolines and Quinazolines^a



^a Reagents and conditions: (a) Pd(PPh₃)₄, aq 1 M NaHCO₃, DME, 80 °C.

The triazine analogues were constructed from commercially available cyanopyridine **16** (Scheme 5). The nitrile was converted to 2-chlorotriazine **20** in 45% overall yield by a four-step sequence: (1) ethanol addition yielded moisture-sensitive imidate **17**, (2) displacement of ethanol with ammonia provided amidine **18**, (3) reaction with cyanamide produced *N*-cyanoamidine **19**, and (4) treatment with POCl₃ and DMF afforded the desired 2-chlorotriazine **20** as an air-stable white solid.²⁰ *N*-Methylamine addition occurred selectively at the more electrophilic triazinyl chloride to provide **21** in 80% yield. This chloride was typically displaced at room temperature, whereas the pyridinyl chloride required temperatures in excess of 80 °C to undergo displacement by amines. Triazine target molecules

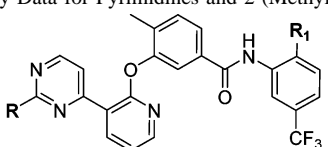
Table 1. Potency Data for Biaryl Anilines and Ethers


Cmpd.	X	R	enzyme inhibition IC ₅₀ (nM)	
			Tie-2	KDR
6	NH		4	4
37	NH		1,220	435
38	NH		504	177
39	NH		1	2
40	NH		43	58
41	NH		181	>25,000
42	O		153	59
43	O		2,700	705
44	O		103	100
45	O		366	1,300

24 and **59–65** (Tables 3 and 5) were provided after further elaboration by analogous reactions described in Schemes 3 and 4.

In the interest of devising multiple synthetic routes to incorporate diversity, direct coupling of the hydroxybenzoic acids (**13**) with anilines was explored (Scheme 5). Standard coupling conditions (HATU, EDC, via acyl chloride) provided little or no desired amide product (**23**), in our hands. Successful coupling of hydroxybenzoic acid **13** with aniline **22** to yield hydroxyamide **23** (45% yield, 1.50 g) was accomplished by a PCl_3 -mediated coupling method.²¹ This protocol provided more satisfactory yields and simplified purification for the amide coupling of certain sterically hindered 2-substituted anilines compared with coupling of the aniline and penultimate intermediate carboxylic acids **12** or **14** (with HATU or via the acid chloride). The derivatized phenol **23** was then coupled to the activated pyridinyl chloride **21** under basic conditions to generate **24**. Target molecules **24** and **49–51** (Table 3) were synthesized by these general synthetic methods.

Other heterocycle variations were synthesized by exploiting chemoselective Suzuki–Miyaura coupling reactions²² of activated iodides and chlorides (Schemes 6 and 7). The 4-iodopyridine **25** selectively reacted with pyridine boronic acid **26** in the presence of $\text{Pd}(\text{OAc})_2$ and $t\text{-Bu}_3\text{P}\cdot\text{HBF}_4$ (biphasic condi-

Table 2. Potency Data for Pyrimidines and 2-(Methylamino)pyrimidines


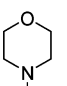
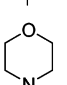
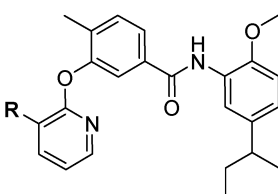
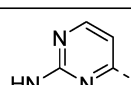
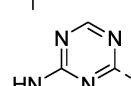
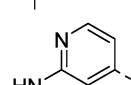
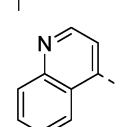
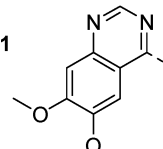
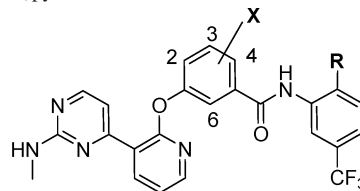
Cmpd.	R	R ₁	enzyme inhibition IC ₅₀ (nM)		cellular inhibition Tie-2 phos IC ₅₀ (nM)
			Tie-2	KDR	
42	H	H	153	59	—
15	MeHN	H	1	3	10
46	H		399	>25,000	—
47	MeHN		10	310	317

Table 3. Potency Data and Rat Iv Clearance Values for Linker-Binding Ring Variations


Cmpd.	R	enzyme inhibition IC ₅₀ (nM)		cellular inhibition Tie-2 phos IC ₅₀ (nM)	Rat iv Clearance (mL/h/kg)
		Tie-2	KDR		
48		4	70	16	3490
24		22	>25,000	61	770
49		62	>25,000	111	5900
50		>25,000	>25,000	—	—
51		>25,000	>25,000	—	—

tions: dioxane/water) to produce the dihalogenated bipyridyl intermediate **27** in 96% yield.²³ The activated fluoride was subsequently displaced by *N*-methylamine in a completely selective fashion over the activated chloride to yield **28** (89%). Quinoline and quinazoline derivatives were accessed by reaction of the corresponding chlorides (**29** and **32**) with boronic acid **30** and a catalytic amount of $\text{Pd}(\text{PPh}_3)_4$ to generate biaryl

Table 4. Potency Data and Rat Iv Clearance Values for 2-(Methylamino)pyrimidines


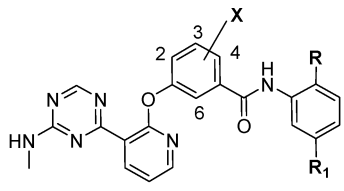
Cmpd.	X	R	enzyme inhibition IC ₅₀ (nM)		cellular inhibition Tie-2 phos IC ₅₀ (nM)	Rat iv Clearance (mL/h/kg)
			Tie-2	KDR		
52	H		99	>8,000	368	3240
53	2-F		62	2,000	105	1533
54	2-Cl		30	675	121	1296
55	2-Me		39	461	462	—
56	6-Me		388	2,600	—	—
57	4-F		40	>25,000	244	340
58	4-F		4	46	46	722

systems **31** and **33**, respectively. Target molecules **49–51** (Table 3) were constructed by the chemistry described in Scheme 5.

Results and Discussion

Structure-Based Design and Structure–Activity Relationships (SAR). We initiated our Tie-2 program by examining a designed scaffold that binds to a broad range of kinases in the “DFG-out” conformation. Kinase inhibitors of the general structural class **6** had emerged by overlay of X-ray cocrystal structures of “DFG-in” binding triazine **34** (IC₅₀'s: Tie-2 = >5000 nM and KDR = 68 nM) and DFG-out binding nicotinamide **35** (IC₅₀'s: Tie-2 = >25 000 nM and KDR = 38 nM) bound to KDR (Figure 2).²⁴ The good overlap of the rings occupying the hydrophobic pocket (HP) in each structure suggested that a hybrid DFG-out binding scaffold could be created by grafting the arylcarboxamide from nicotinamide **35** onto triazine **34** (Figure 2b). The resulting oversized compound **36** (molecular weight = 642 g/mol) exhibited potency against Tie-2 (IC₅₀ = 85 nM) and KDR (IC₅₀ = 38 nM) enzymes. Trimming molecular weight from the structure produced compounds such as **6** (Figures 1 and 2b), which inhibited a broad range of kinases including Tie-2 (IC₅₀ = 4 nM) and KDR (IC₅₀ = 4 nM) enzymes.

Our first goal was to introduce selectivity over other kinases, especially those involved in angiogenesis, e.g., KDR, into our

Table 5. Potency Data and Rat Iv Clearance Values for 2-(Methylamino)triazines


Cmpd.	X	R	R ₁	enzyme inhibition IC ₅₀ (nM)		cellular inhibition Tie-2 phos IC ₅₀ (nM)	Rat iv Clearance (mL/h/kg)
				Tie-2	KDR		
59	2-Me	H	CF ₃	10	97	38	—
60	2-Me		CF ₃	108	>25,000	810	6100
61	2-Me		CF ₃	59	4,000	140	921
62	4-F		CF ₃	53	>25,000	852	—
63	4-F		CF ₃	30	7,800	62	1300
64	4-F		i-Pr	6	>8,000	25	4200
65	4-F		c-Pr	13	>25,000	39	2730

initial potent Tie-2 inhibitors. All kinase assays were run at the *K_m* for ATP (Tie-2 = 5 μM ATP; KDR = 1 μM ATP) and quenched within the linearity of the enzyme. All enzyme data described were an average of two determinations, and the Tie-2 data were commonly an average of four determinations. The aniline fragment of the molecule (**R**-group) preferred a lipophilic group, such as trifluoromethyl, in the 3-position for enzyme potency, e.g., **6** (Table 1). Removing this substituent (**37**) or moving it to the 4-position (**38**) rendered the molecule considerably less active against Tie-2 and KDR. After locking the trifluoromethyl group into the 3-position, SAR studies revealed that incorporating groups meta to the trifluoromethyl (**39**) did not affect potency or selectivity against Tie-2 or KDR. Placing a methoxy moiety para to the trifluoromethyl (**40**) resulted in approximately a 10-fold decrease in potency on Tie-2 and KDR. By increasing the bulk of the 2-substituent from methoxy (**40**) to piperidinyl (**41**), reasonable potency was maintained (Tie-2 IC₅₀ = 181 nM) and selectivity over KDR (>100-fold) was achieved.

A drawback to this class of biaryl anilines was the reduced solubility in aqueous and organic media (including DMSO), consistent with the high melting points observed (e.g., **38**; 0.001 mg/mL in 0.01 N HCl, mp = 268–270 °C). By changing the biaryl aniline (e.g., **6**) to a biaryl ether (e.g., **42**; Table 1), we eliminated the strong intramolecular hydrogen bond between the aniline and the adjacent pyrimidine nitrogen.²⁵ The resulting compounds were lower melting, white solids with improved solubility in organic solvents and a modest improvement in aqueous media (e.g., **43**; 0.005 mg/mL in 0.01 N HCl, mp = 190–193 °C). The cost of this improvement in physical

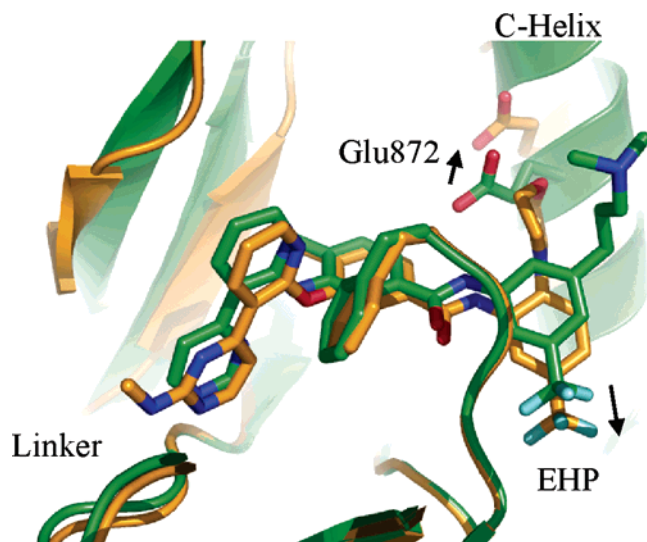


Figure 3. X-ray cocrystal structures of pyrimidine **39** (green) and 2-(methylamino)pyrimidine **47** (brown) bound to the ATP binding site of Tie-2 (oxygen atoms = red, nitrogen atoms = blue, fluorine atoms = light blue). Compounds **39** and **47** bind the linker residues in a very similar fashion. The bulky morpholino substituent of **47** pushes Glu872 of the α C-helix out by approximately 3.5 Å relative to the structure of **39**.

properties was a 2–40-fold loss in Tie-2 enzyme potency (e.g., **42** vs **6**). The reason for the reduced potency for the biaryl ether series was not clear from comparing X-ray cocrystal structures (see superimposition of **39** and **47** in Figure 3). Fortunately, the trends in KDR selectivity still translated qualitatively to the biaryl ether series (e.g., **41** vs **45**).

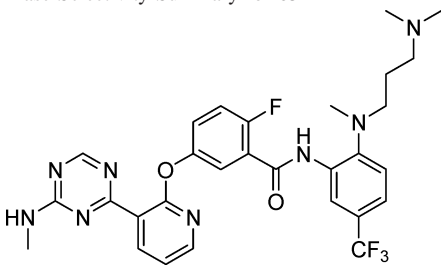
To address the compromised potency in the biaryl ether class (**42**–**45**), we turned our attention to enhancing binding of the ligand to the protein via an additional hydrogen bond with the hinge region (linker) of the kinase. Traditionally, kinase inhibitors possess a hydrogen-bond donor/acceptor/donor motif to best interact with the backbone carbonyl/amide NH/carbonyl presented by the protein in the ATP-binding cleft.²⁶ In the case of Tie-2, these residues are Ala905 (carbonyl and amide NH) and Glu903 (carbonyl). In contrast, the KDR hinge region residues are Cys919 (carbonyl and amide NH) and Glu917 (carbonyl). The pyrimidine N1 of **42** was making a significant hydrogen bond only with the Ala905 amide NH. With an amino group in the 2-position of the pyrimidine, a hydrogen bond was predicted to exist with the Ala905 carbonyl, in addition to the pyrimidine nitrogen/Ala905 amide NH hydrogen bond. This hypothesis was evaluated by preparing 2-methylamino derivatives **15** and **47**, and their potency and KDR selectivity were compared to the nor-methylamino derivatives **42** and **46**, respectively (Table 2). Indeed, the additional binding element provided a 40–150-fold boost in potency at the Tie-2 receptor. The binding affinity of **15** was comparable to that of the analogous biaryl aniline **6** (Tie-2 IC_{50} = 1 and 4 nM, respectively). Disappointingly, there were no improvements in selectivity vs KDR. At the cellular level, **15** inhibited Tie-2 phosphorylation with an IC_{50} of 10 nM. The 2,5-disubstituted derivative **47** was less cell active (IC_{50} = 317 nM) with a 30-fold enzyme to cell potency shift.

We were fortunate to obtain X-ray cocrystal structures of **39** (green) and **47** (brown) bound to the ATP site of the Tie-2 kinase domain (Figure 3). These molecules bind in a very similar manner and induce the inactive DFG-out conformation of the protein, as expected (see Figure 2).^{27,28} The pyrimidine ring N1 nitrogen acceptor of **39** resides 2.9 Å from the linker residue

Ala905 backbone NH making an ideal single hydrogen bond. Two further interactions from the pyrimidine include van der Waals contact with two backbone carbonyls via its CH's in the 2- and 6-position. In contrast, the 2-(methylamino)pyrimidine ring (**47**) binds to the linker residue Ala905 via two hydrogen bonds, as predicted: donor distance of 3.0 Å (MeNH) and acceptor at 2.8 Å (N). The pyrimidine 6-CH is also within van der Waals contact (3.7 Å) of the Glu903 backbone carbonyl (Figure 3).²⁹ In both cases, the pyridine ring serves to position the pyrimidine ring within H-bonding distance to the linker residues and place the central methyl-substituted aryl ring in the first hydrophobic pocket (HP). Additionally, the pyridine ring forms an edge-to-face π -stacking interaction with Phe983 of the DFG-motif (\sim 3.5 Å). The aryl amide moiety directs the terminal CF₃-substituted aromatic ring into the extended hydrophobic pocket (EHP), and the carbonyl oxygen makes a hydrogen bond with the backbone NH of Asp982 (DFG motif). To our surprise, a hydrogen bond between the amide NH and the Glu872 side chain (located on the α C-helix), present in the structure of **39** and thought to be important for potency, was absent for **47**. Instead, the morpholino residue pushed the α C-helix approximately 3.5 Å from its normal position, as observed for **39**, and forced the trifluoromethyl group deeper into the extended hydrophobic pocket relative to its position in the structure of **39**. This data led us to speculate that Tie-2 is more flexible in this region than KDR, resulting in modest to excellent selectivity.

In the 2-(methylamino)pyrimidine series, the 2-methoxy-5-cyclohexylaniline analogue **48** provided improved cellular potency (IC_{50} = 16 nM, Table 3) relative to the 2-morpholino-5-CF₃ aniline **47** (IC_{50} = 310 nM, Table 2), at the expense of reduced selectivity against KDR. One avenue we explored to improve the selectivity was modification of the linker-binding ring (Table 3). Triazine **24** and pyridine **49** provided excellent selectivity over KDR but inadequate cellular potency. Rat iv pharmacokinetic studies further revealed a very short mean residence time (MRT = 0.47 h) for **24** and very high clearance for **49**. Interestingly, bulkier quinoline **50** and dimethoxyquinazoline **51** showed insufficient Tie-2 and KDR enzyme activity.

Continued SAR studies of the pyrimidine series involved changing the location and size of the hydrophobic substituent on the central aryl ring that occupies the first hydrophobic pocket of Tie-2 (Table 4). Keeping the terminal aryl ring constant as a 2-piperidine-5-trifluoromethylphenyl group, the central ring modifications were evaluated with respect to cellular potency and in vivo clearance. Compounds bearing no substitution (**52**) or 2-substitution (**53**–**55**) exhibited moderate cellular activity (105–462 nM) but iv clearances of greater than 1250 mL/h/kg. A methyl group in the 6-position (**56**) resulted in a significant loss in Tie-2 enzyme potency. By moving a fluorine atom from the 2-position (**53**) to the 4-position (**57**), a 2.5-fold reduction in cellular potency was accompanied by improved KDR selectivity and a dramatic reduction in the in vivo clearance (clearance = 1533 vs 340 mL/h/kg). Unfortunately, the cellular potency for **57** was still inadequate to warrant evaluation in a pharmacodynamic model. We next changed the piperidinyl group to a more flexible, yet still bulky, linear alkyl diamine **58**. As expected, a reduction in the rigidity of the 2-substituent on the terminal aryl ring led to an improvement in cell potency at the cost of KDR selectivity (11-fold for **58** vs >500-fold for **57**). To our surprise, the in vivo clearance of tertiary amine **58**

Table 6. Kinase Selectivity Summary for **63**


The chemical structure of compound 63 features a central triazine ring substituted with a methylamino group (NHMe) and a 2-pyridylmethyl group. This triazine is linked via an oxygen atom to a 4-fluorophenyl ring, which is further substituted with a trifluoromethyl group (CF₃) and an amide linkage (-NH-) to a 4-(dimethylamino)phenyl ring.

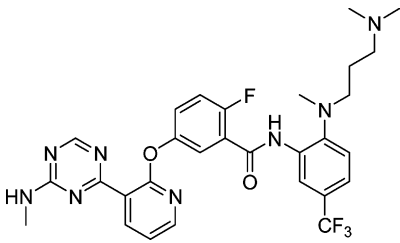
enzyme inhibition IC ₅₀ (nM)		
Tie-2: 30	SYK: 25 000	p38α: 3 700
KDR: 7 800	Zap70: 25 000	JNK3: 40 000
PDGFR: 1 940	Jak3: 25 000	CDK5: 100 000
cfms: 25 000	CSK: 25 000	AurA: 25 000
RET: 8 300	Src: 5 750	PKBα: 100 000
TrkA: 8 300	Lck: 1 100	
cMet: 25 000	Lyn: 4 900	
EGFR: 25 000	Fgr: 8 300	
INSR: 4 200	Abl: 1 280	
IGFR-1: 927	BTK: 25 000	
EpHB4: 8 300	Itk: 25 000	
	Fes: 25 000	

was an acceptable 722 mL/h/kg. Furthermore, the oral bioavailability of **58** at 32% proved to be better than that of **57** ($F = 0.3\%$).

Concurrent with SAR studies in the pyrimidine series, we explored triazine analogues (Table 5). In general, the 2-(methylamino)triazine linker-binding group provided the improved selectivity for Tie-2 over KDR that was elusive in the pyrimidine series (e.g., triazine **59** vs pyrimidine **15**). The origin of this significant difference in selectivity resulting from a minor change of a CH (pyrimidine) to a N (triazine) linker-binding group was not readily apparent from an X-ray structural perspective. Fortunately, as in the pyrimidine case, changing the piperidinyl group to the linear alkyl diamine chain in the triazine series provided a significant increase in cellular potency (**60** vs **61** and **62** vs **63**). The 4-fluoro vs 2-methyl substitution in conjunction with the flexible bulk of a diamine side chain (**63** vs **61**) resulted in a 2.3-fold improvement in cellular potency and maintained modest iv clearance.

The final SAR studies were directed at optimizing the lipophilic trifluoromethyl moiety on the terminal aryl ring. Improved cellular potency was obtained with isopropyl substituted **64** at the expense of increased in vivo clearance (Table 5). Switching this group to a cyclopropyl ring (**65**), in hopes of decreasing clearance, once again showed improved cellular potency but over twice the in vivo clearance of **63**. Our optimization studies culminated in identifying compound **63**, with the best balance of desired properties (potency, selectivity, and iv clearance) for further investigation.

Kinase Selectivity. In extensive kinase screening, **63** displayed remarkably high selectivity over a wide range of phylogenetically diverse tyrosine and serine/threonine kinases (Table 6). Particularly important was the pronounced specificity over other kinases known to be involved in angiogenesis, such as KDR (>250-fold, IC₅₀ = 7800 nM), PDGFR (>60-fold, IC₅₀ = 1940 nM), and EpHB4 (>275-fold, IC₅₀ = 8300 nM). IGFR-1 was the single kinase screened that resulted in submicromolar potency (IC₅₀ = 927 nM), equating to a minimum selectivity of 30-fold for **63** for the Tie-2 kinase across the broad panel. By combining key structural features, namely, the triazine linker-binding ring, 4-fluoro substitution of the central aryl ring,

Table 7. Physicochemical Properties and Pharmacokinetic/Drug Metabolism Measurements for **63**


The chemical structure of compound 63 is identical to the one shown in Table 6.

physicochemical properties	solubility (mg/mL)
MW: 598.6	0.01 N HCl: 1.32
cLogP: 4.8	SIF: 0.34
PSA: 108	PBS: 0.044
pK _a : 9.5	

rat pharmacokinetics ^a	protein binding
<i>T</i> _{1/2} : 1.6 h	rat: 93.0%
Cl: 1300 mL/h/kg	mouse: 98.0%
<i>V</i> _{ss} : 2560 mL/kg	human: 92.2%
<i>F</i> : 31%	
<i>C</i> _{max} : 520 ng/mL	
AUC _{0-∞} : 2640 ng h/mL	

^a Dosed intravenously at 1 mg/kg in DMSO and orally at 10 mg/kg in OraPlus (pH = 2.2) to male Sprague–Dawley rats ($N = 3$ animals for all pharmacokinetic data).

and 2,5-substitution of the terminal aryl ring, a highly Tie-2 specific molecule was realized.

In Vivo Profile. Compound **63** was initially selected on the basis of potency, selectivity, and a reasonable rat pharmacokinetic (PK) profile when dosed intravenously (1 mg/kg). The iv data revealed modest clearance and volume of distribution and an acceptable half-life of 1.6 h (Table 7). When dosed orally at 10 mg/kg, 31% bioavailability was achieved with a *C*_{max} of 520 ng/mL being reached 2 h postdose (*T*_{max}). Although this molecule has a high molecular weight (598.6 g/mol), both the cLogP (4.8) and PSA (108) are within generally acceptable ranges for orally administered agents.³⁰ The measured solubility of **63** was excellent in 0.01 N HCl and simulated intestinal fluid (SIF, pH = 6.8), likely due to the basicity of the tertiary amine and moderate in phosphate buffer solution (PBS, pH = 7.0). It was also encouraging that the measured protein binding in rat, mouse, and human was 93.0%, 98.0%, and 92.2%, respectively, ensuring adequate free fraction of compound in all three species.

The ability of **63** to modulate Tie-2 phosphorylation levels in vivo was measured in a mouse pharmacodynamic model over a 12 h time period (Figure 4). The compound was administered po at 100 mg/kg at time zero. Angiopoietin-1 was administered intravenously 15 min before the 3, 8, and 12 h time points. Mouse lungs were then harvested and the levels of phosphorylated Tie-2 were measured by Western blot analysis, and plasma concentrations of compound were determined (single study, $N = 3$ animals/group). At the 3 h time point, $3.97 \pm 0.42 \mu\text{M}$ plasma concentration was achieved, and phosphorylated Tie-2 levels were reduced by 94% ($p = 0.0002$) with respect to basal (vehicle). By the 8 h time point, the amount of phosphorylated Tie-2 (reduced 25% with respect to basal; $p = 0.349$) had nearly returned to the Ang-1-stimulated control level ($3.03 \pm 0.45 \mu\text{M}$ plasma concentration of **63**). These data suggest that a 100 mg/kg dose will provide some target coverage in an in vivo setting for several hours and that a multiple oral dosing regimen would be required for sustained inhibition of Tie-2 phosphorylation in the mouse.

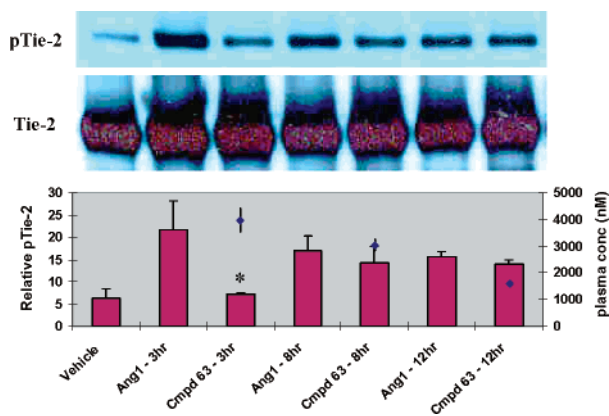


Figure 4. Compound **63** inhibits Ang-1 stimulated Tie-2 phosphorylation measured in mouse lungs, as analyzed by IP-Western analysis at a 100 mg/kg po dose (mean pTie-2 levels illustrated as bars). Total Tie-2 levels remain constant throughout the experiment. With respect to basal, a 94% reduction in phosphorylation level was achieved at the 3 h time point ($3.97 \pm 0.42 \mu\text{M}$ plasma concentration of **63**; mean plasma concentrations illustrated as diamonds). $N = 3$ animals per dosing group. * $p < 0.0167$ vs Ang-1 stimulated control. Statistical analysis was performed by one-way ANOVA with Fishers posthoc test adjusted manually for three comparisons ($p = 0.0002$).

Conclusion

A novel set of Tie-2 inhibitors based on pyridinyl pyrimidine and pyridinyl triazine scaffolds has been described in detail. Interaction of the target protein with ligand was determined from X-ray structures. This information guided the medicinal chemistry direction in the lead optimization stage of this program. Utilizing both classical heterocyclic chemistry and modern catalyst systems for Suzuki–Miyaura couplings, advanced intermediates were generated in multigram quantities. By systematic variation of all groups around the pyridine core, comprehensive SAR studies led to a highly selective, cell potent, and orally bioavailable Tie-2 inhibitor (**63**). Compound **63** demonstrated good pharmacokinetic properties when administered by iv and po routes. This compound was potent in a Tie-2 autophosphorylation cellular assay ($\text{IC}_{50} = 62 \text{ nM}$) and possessed >30-fold selectivity over all kinases screened in enzyme assays. It reduced the amount of phosphorylated Tie-2 by 94% with respect to basal at the 3 h time point in a mouse pharmacodynamic study (Ang-1-stimulated phosphorylated Tie-2) when dosed orally at 100 mg/kg. The tremendous selectivity and adequate cellular potency and PK properties of **63** enable it to function as a tool to better understand the role Tie-2 plays in angiogenesis and tumor progression.

Experimental Section

Unless otherwise noted, all materials were obtained from commercial suppliers and used without further purification. Compounds **40**, **52**, **53**, **54**, **56**, and **59** were obtained from Polyphor LTD, Allschwil, Switzerland. Anhydrous solvents were obtained from Aldrich and used directly. All reactions involving air- or moisture-sensitive reagents were performed under a nitrogen or argon atmosphere. Silica gel chromatography was performed using either glass columns packed with silica gel (200–400 mesh, Aldrich Chemical) or medium-pressure liquid chromatography (MPLC) on a CombiFlash Companion (Teledyne Isco) with RediSep normal-phase silica gel (35–60 μm) columns and UV detection at 254 nm. Preparative reversed-phase HPLC was performed on a Gilson (215 liquid handler), YMC-Pack Pro C18, 150 \times 30 mm i.d. column, eluting with a binary solvent system using a gradient elution (A, H_2O with 0.1% TFA; B, CH_3CN with 0.1% TFA) with UV detection at 254 nm. Melting points were obtained using an OptiMelt and are uncorrected. All final compounds were purified

to >95% purity as determined by high performance liquid chromatography (HPLC) with an Agilent 1100 Series instrument and UV detection at 254 nm (system A, Zorbax SB-C8, $4.6 \times 150 \text{ mm}$, 15 min, 1.5 mL/min flow rate, from 0 to 100% 0.1% TFA in CH_3CN /from 100 to 0% 0.1% TFA in H_2O ; system B, Phenomenex Synergi, $2 \times 50 \text{ mm}$, 3 min, 1.0 mL/min flow rate, from 5 to 95% 0.1% formic acid in CH_3CN /from 95 to 5% 0.1% formic acid in H_2O ; system C, Zorbax SB-C8, $4.6 \times 75 \text{ mm}$, 12 min, 1.0 mL/min flow rate, from 10 to 90% 0.1% formic acid in CH_3CN /from 90 to 10% 0.1% formic acid in H_2O). NMR spectra were determined with either a Bruker AV-400 (400 MHz) spectrometer or a Varian 400 or 300 MHz spectrometer at ambient temperature. Low-resolution mass spectral (MS) data were determined on an Agilent 1100 Series LCMS with UV detection at 254 nm and a low resonance electrospray mode (ESI). Chemical shifts are reported in ppm from the solvent resonance ($\text{DMSO}-d_6$, 2.49 ppm). Data are reported as follows: chemical shift, multiplicity (s = singlet, d = doublet, t = triplet, q = quartet, br = broad, m = multiplet), coupling constants, and number of protons. High-resolution mass spectra (HRMS) were obtained on a high-resolution electrospray time-of-flight mass spectrometer. Combustion analysis was performed by Galbraith Laboratories, Inc., Knoxville, TN.

1-(2-Chloropyridin-3-yl)-3-dimethylaminopropenone (8). 1-(2-Chloropyridin-3-yl)ethanone (**7**)¹⁹ (21.7 g, 139 mmol) in *N,N*-dimethylformamide dimethyl acetal (42.0 g, 46.0 mL, 350 mmol) was heated under a drying tube at 85 °C for 1.5 h and concentrated. The residue was purified by suction filtration chromatography (using 150 g of silica gel in a Buchner funnel, with rapid collection of fractions eluting with 10:1 and then 5:1 CH_2Cl_2 /2-propanol) to provide 16.1 g (56%) of a yellow solid: ^1H NMR (400 MHz, $\text{DMSO}-d_6$) δ 8.42 (d, $J = 4 \text{ Hz}$, 1H), 7.77 (br s, 1H), 7.46 (dd, $J = 4, 8 \text{ Hz}$, 1H), 5.25 (d, $J = 12 \text{ Hz}$, 1H), 3.10 (s, 3H), 2.86 (s, 3H); MS, m/z ($\text{C}_{10}\text{H}_{11}\text{ClN}_2\text{O}$) calcd 210.66, found 211 (MH).

4-(2-Chloropyridin-3-yl)pyrimidine (9). Sodium methoxide was generated over a period of 1.5 h by the intermittent addition of small chunks of sodium metal (8.30 g, 360 mmol) to dry methanol (400 mL) under N_2 at room temperature, using a bath of 500 mL of 2-propanol at room temperature as a heat sink. Formamidinium acetate (42.7 g, 410 mmol) was added, followed 10 min later by **8** (30.6 g, 146 mmol). The reaction was stirred overnight under a N_2 -filled balloon at an internal temperature of 40 °C. After 20 h, the mixture was stirred at 48 °C for 4 h. Additional formamidinium acetate (7.0 g, 67 mmol) was added and the mixture was stirred overnight at 44 °C. The mixture was concentrated by rotary evaporator, taken up in ethyl acetate, and extracted with saturated aqueous NaHCO_3 . The aqueous layer was back-extracted with EtOAc. The combined organic layers (1.2 L) were dried over Na_2SO_4 and concentrated. The residue was purified by flash vacuum filtration chromatography (300 g silica gel) in 3:1 to 2:1 hexane/EtOAc to provide 23.2 g (83%) of a white solid: ^1H NMR (400 MHz, $\text{DMSO}-d_6$) δ 9.21 (s, 1H), 8.84 (d, $J = 4 \text{ Hz}$, 1H), 8.44 (d, $J = 4 \text{ Hz}$, 1H), 8.01 (dd, $J = 4, 8 \text{ Hz}$, 1H), 7.81 (d, $J = 4 \text{ Hz}$, 1H), 7.50 (dd, $J = 4, 8 \text{ Hz}$, 1H).

4-(2-Chloropyridin-3-yl)-*N*-methylpyrimidin-2-amine (10). Sodium metal (3.40 g, 148 mmol) was added over ~ 10 min to MeOH (180 mL) at room temperature and allowed to stir for an additional 30 min to generate sodium methoxide. *N*-Methylguanidine·HCl (20.0 g, 182 mmol) was added and the resulting mixture was stirred for 30 min before **8** (12 g, 57 mmol) was added. An air condenser was attached and the mixture was heated to 50 °C for 23 h. After cooling, part of the MeOH was removed by rotary evaporation and the resulting solid was filtered and washed with saturated aqueous NaHCO_3 and water. The desired product was obtained as a fluffy white solid (11.4 g, 90%): ^1H NMR (400 MHz, $\text{DMSO}-d_6$) δ 8.51 (dd, $J = 1.6, 4.8 \text{ Hz}$, 1H), 8.41 (br s, 1H), 8.04 (br s, 1H), 7.57 (dd, $J = 4.8, 7.6 \text{ Hz}$, 1H), 7.32 (m, 1H), 6.87 (m, 1H), 2.82 (d, $J = 4.8 \text{ Hz}$, 3H); MS, m/z ($\text{C}_{10}\text{H}_9\text{ClN}_4$) calcd 220.66, found 221 (MH).

4-Methyl-3-(3-pyrimidin-4-ylpyridin-2-ylamino)benzoic Acid (12). 4-(2-Chloropyridin-3-yl)pyrimidine (**9**) (10.4 g, 54 mmol), **11** (19.4 g, 128 mmol), $\text{Et}_3\text{N}\cdot\text{TFA}$ salt (17 g, the liquid $\text{Et}_3\text{N}\cdot\text{TFA}$

reagent was generated by adding 2.5 mL of TFA dropwise to a 0 °C solution of 3 mL Et₃N in 2-propanol and then concentrating by rotary evaporator followed by 30 min under high vacuum, and DMSO (15 mL) were mixed together in a sealed tube under argon. The mixture was stirred at 95 °C for 65 h. After cooling to room temperature, the residue was sonicated in 100 mL of methanol to break up the solids and then filtered to obtain 11.7 g (71%) of product as a yellow solid: ¹H NMR (300 MHz, DMSO-*d*₆) δ 12.57 (s, 1H), 11.58 (s, 1H), 9.21 (s, 1H), 8.77 (d, *J* = 5.5 Hz, 1H), 8.74 (s, 1H), 8.32 (d, *J* = 7.6 Hz, 1H), 8.21 (m, 1H), 8.10 (dd, *J* = 1.1, 5.5 Hz, 1H), 7.37 (d, *J* = 7.5 Hz, 1H), 7.19 (d, *J* = 7.5 Hz, 1H), 6.83 (dd, *J* = 4.7, 7.9 Hz, 1H), 2.31 (s, 3H).

4-Methyl-3-(3-(pyrimidin-4-yl)pyridin-2-ylamino)-*N*-(3-(trifluoromethyl)phenyl)benzamide (6). 4-Methyl-3-(3-pyrimidin-4-ylpyridin-2-ylamino)benzoic acid (**12**) (106 mg, 0.340 mmol) was suspended in DMF (1.5 mL). EDC (86 mg, 0.44 mmol) and DMAP (42 mg, 0.35 mmol) were added, and the mixture was stirred at 60 °C for 10 min. After cooling, 3-trifluoromethylaniline (111 mg, 0.690 mmol) was added to the mixture, which was then stirred under N₂ at 85 °C for 8 h. Concentration, trituration with methanol, and filtration provided 99 mg (65%) of product as a yellow solid: ¹H NMR (300 MHz, DMSO-*d*₆) δ 11.57 (s, 1H), 10.31 (s, 1H), 9.23 (s, 1H), 8.78 (d, *J* = 5.1 Hz, 1H), 8.68 (s, 1H), 8.35 (d, *J* = 7.8 Hz, 1H), 8.21 (m, 1H), 8.11 (s, 2H), 7.89 (d, *J* = 7.5 Hz, 1H), 7.44 (m, 2H), 7.27 (m, 2H), 6.85 (m, 1H), 2.32 (s, 3H); HPLC purity = 99% (system A), 100% (system C); HRMS (C₂₄H₁₈F₃N₅O)⁺ calcd 450.15362, found 450.15532.

4-Methyl-3-(3-(2-(methylamino)pyrimidin-4-yl)pyridin-2-yloxy)benzoic Acid (14). To 4-(2-chloropyridin-3-yl)-*N*-methylpyrimidin-2-amine (**10**) (4.00 g, 18.1 mmol), **13** (2.90 g, 19.0 mmol), and cesium carbonate (11.8 g, 36.2 mmol) was added DMSO (20 mL). The mixture was heated in an argon-purged sealed tube to 130 °C for 16 h. The cooled mixture was diluted with water and extracted with EtOAc. The aqueous layer was neutralized with TFA (pH ~ 7) and the resulting solid was filtered and washed with water and diethyl ether to yield 5.31 g (87%) of the desired product as an off-white solid: ¹H NMR (300 MHz, DMSO-*d*₆) δ 8.48 (br s, 1H), 8.38 (d, *J* = 4.4 Hz, 1H), 8.17 (dd, *J* = 1.6, 4.8 Hz, 1H), 7.72 (d, *J* = 7.6 Hz, 1H), 7.56 (s, 1H), 7.42 (d, *J* = 7.6 Hz, 1H), 7.30 (m, 2H), 7.21 (m, 1H), 2.87 (d, *J* = 4.4 Hz, 3H), 2.15 (s, 3H).

4-Methyl-3-(3-(2-(methylamino)pyrimidin-4-yl)pyridin-2-yloxy)-*N*-(3-(trifluoromethyl)phenyl)benzamide (15). 4-Methyl-3-(3-(2-(methylamino)pyrimidin-4-yl)pyridin-2-yloxy)benzoic acid (**14**) (30 mg, 0.067 mmol) and HATU (38 mg, 0.10 mmol) were dissolved in DMF (1.2 mL). 3-Trifluoromethylaniline (0.013 mL, 0.10 mmol) and DIPEA (0.030 mL, 0.17 mmol) were added, and the reaction was heated to 80 °C for 2 h. The crude reaction was purified by Gilson reverse-phase HPLC. The product-containing fractions were diluted with methylene chloride and extracted with saturated sodium bicarbonate. The organic layer was dried over anhydrous sodium sulfate, filtered, and concentrated to yield 20 mg (63%) of product as a white solid: ¹H NMR (300 MHz, DMSO-*d*₆) δ 10.44 (s, 1H), 8.48 (br s, 1H), 8.38 (d, *J* = 5.1 Hz, 1H), 8.17 (m, 2H), 8.05 (d, *J* = 7.8 Hz, 1H), 7.83 (dd, *J* = 1.8, 7.8 Hz, 1H), 7.75 (d, *J* = 1.8 Hz, 1H), 7.57 (m, 1H), 7.50 (d, *J* = 7.8 Hz, 1H), 7.41 (d, *J* = 7.8 Hz, 1H), 7.30 (m, 2H), 7.21 (m, 1H), 2.88 (d, *J* = 4.5 Hz, 3H), 2.18 (s, 3H); HPLC purity = 98% (system A), 100% (system C); HRMS (C₂₅H₂₀F₃N₅O₂)⁺ calcd 480.16419, found 480.16368.

Alternative Procedure. Compound **14** was treated with oxalyl chloride (1.0 equiv) and a catalytic amount of DMF in CH₂Cl₂ (0.1 M) at 0 °C. The mixture was stirred at room temperature for 3.5 h and concentrated to yield the desired acid chloride·HCl salt as a yellowish solid. This material was further reacted without purification with anilines (1.0 equiv) in THF (0.1 M) at room temperature for approximately 24 h to yield desired products similar to **15** (15–80% yields).

2-Chloronicotinamide (18).²⁰ 2-Chloro-3-cyanopyridine (**16**) (5.0 g, 36 mmol) was dissolved in dry EtOH (100 mL) at 0 °C. HCl was bubbled through the mixture for 3 h and the mixture was sealed and refrigerated (about 8 °C) overnight. After concentration, the residue (**17**) was stirred at room temperature with ammonium

acetate (5.5 g, 71 mmol) in 2-propanol (100 mL). After 12 h, the pH was adjusted to 9 (from 4) using concentrated NH₄OH solution and stirring continued two more days. The mixture was concentrated and purified by flash chromatography (10:1:0.1 CH₂Cl₂/MeOH/NH₄OH). Trituration in hot *t*-BuOMe/2-propanol removed some residual amide side product to provide 3.64 g (65%) of the product as a white solid. This material was used without further purification: MS, *m/z* (C₆H₆ClN₃) calcd 155.59, found 155 (M).

Amino-(2-chloropyridin-3-yl)methylcyanamide (19).²⁰ 2-Chloronicotinamide (**18**) (11.7 g, 75.2 mmol) was suspended in 2-propanol (10 mL), and cyanamide (6.7 g, 160 mmol) was added. The mixture was stirred as a 0.6 M solution of NaHCO₃ (60 mL) was added until the reaction was homogeneous and the pH was 9. After 2 days of stirring, 11.3 g (83%) of the product was isolated by EtOAc extraction of the aqueous reaction mixture followed by flash chromatography using 95:5:0.5 CH₂Cl₂/MeOH/NH₄OH. This material was used without further purification: MS, *m/z* (C₇H₆ClN₄) calcd 181.03, found 181 (M).

2-Chloro-4-(2-chloropyridin-3-yl)-[1,3,5]triazine (20). Amino-(2-chloro-pyridin-3-yl)methylcyanamide (**19**) (3.5 g, 19 mmol) was added as a solid to a stirring, 0 °C solution of POCl₃ (2.3 mL, 25 mmol) and DMF (1.9 mL, 25 mmol) in acetonitrile (100 mL). The clear solution was stirred at room temperature for 1 h. Toluene (40 mL) was added and the mixture was concentrated. The residue was immediately filtered through a 200-g plug of silica (loading in 10:1 CH₂Cl₂/2-propanol, eluting with 10:1 to 4:1 hexane/*t*-BuOMe). Concentration provided 3.7 g (84%) of the desired product as a white solid: ¹H NMR (400 MHz, DMSO-*d*₆) δ 9.46 (s, 1H), 8.67 (d, *J* = 4 Hz, 1H), 8.37 (d, *J* = 8 Hz, 1H), 7.68 (dd, *J* = 4, 8 Hz, 1H); MS, *m/z* (C₈H₄Cl₂N₄) calcd 225.98, found 227 (MH).

[4-(2-Chloropyridin-3-yl)-[1,3,5]triazin-2-yl]methylamine (21). To 2-chloro-4-(2-chloro-pyridin-3-yl)-[1,3,5]triazine (**20**) (10.0 g, 44.0 mmol) in methylene chloride (55 mL) was added *N*-methylamine (45.0 mL, 88.0 mmol, 2.0 M in THF) at 0 °C. After stirring at room temperature for 18 h, the mixture was filtered to isolate the resulting solids. The solids were dissolved in 10% NEt₃/EtOAc, filtered through a plug of silica gel, and concentrated to yield the desired product as a white solid (7.8 g, 80%): ¹H NMR (400 MHz, DMSO-*d*₆, two inseparable isomers present in equal amounts in DMSO) isomer 1, δ 8.72 (s, 1H), 8.55 (m, 1H), 8.31 (br m, 1H), 8.21 (d, *J* = 7.6 Hz, 1H), 7.57 (m, 1H), 2.87 (d, *J* = 4.8 Hz, 3H); isomer 2, δ 8.61 (s, 1H), 8.55 (m, 1H), 8.31 (br m, 1H), 8.11 (d, *J* = 7.6 Hz, 1H), 7.57 (m, 1H), 2.86 (d, *J* = 4.8 Hz, 3H).

***N*-(5-Cyclohexyl-2-methoxyphenyl)-3-hydroxy-4-methylbenzamide (23).** 3-Hydroxy-4-methylbenzoic acid (**13**) (1.63 g, 10.7 mmol), 5-cyclohexyl-2-methoxybenzamide (**22**) (2.00 g, 9.74 mmol), and DMAP (400 mg, 3.22 mmol) were suspended in 40 mL of dry toluene in a two-neck flask with an attached Dean–Stark trap under N₂. The mixture was stirred in a 130 °C oil bath and brought to a boil before PCI₃ (0.42 mL, 4.9 mmol) was added dropwise over 15 min. Heating was continued an additional 20 min. After cooling, the mixture was diluted with brine and ethyl acetate and acidified with 1 N HCl. After extraction, the organic layer was dried with Na₂SO₄ and concentrated. The isolated material was packed into a small filtration apparatus and rinsed with a small amount of CH₂Cl₂ to provide the product as a white solid (1.50 g, 45%): ¹H NMR (400 MHz, DMSO-*d*₆) δ 9.68 (s, 1H), 9.08 (s, 1H), 7.75 (s, 1H), 7.33 (s, 1H), 7.30 (d, *J* = 7.8 Hz, 1H), 7.21 (d, *J* = 7.8 Hz, 1H), 6.98 (s, 2H), 3.81 (s, 3H), 2.43 (m, 1H), 2.18 (s, 3H), 1.78 (m, 4H), 1.71 (m, 1H), 1.36 (m, 4H), 1.23 (m, 1H).

***N*-(5-Cyclohexyl-2-methoxyphenyl)-4-methyl-3-(3-(4-(methylamino)-1,3,5-triazin-2-yl)pyridin-2-yloxy)benzamide (24).** To 4-(2-chloropyridin-3-yl)-*N*-methyl-1,3,5-triazin-2-amine (**21**) (0.080 g, 0.36 mmol), *N*-(5-cyclohexyl-2-methoxyphenyl)-3-hydroxy-4-methylbenzamide (**23**) (0.15 g, 0.43 mmol), and cesium carbonate (0.24 g, 0.72 mmol) was added DMSO (0.7 mL). The mixture was heated to 130 °C for 21.5 h. Water was added and the resulting solid was filtered, washed with water, and dried before being purified by Gilson reverse-phase HPLC. The product was diluted with CH₂Cl₂ and extracted with saturated sodium bicarbonate. The

organic layer was dried over anhydrous sodium sulfate, filtered, and concentrated to yield the desired product (103 mg, 54%) as an off-white solid: ^1H NMR (400 MHz, two inseparable isomers present in DMSO- d_6), isomer 1, δ 9.35 (s, 1H), 8.63 (s, 1H), 8.23 (m, 2H), 8.13 (m, 1H), 7.74 (s, 1H), 7.65 (m, 1H), 7.55 (m, 1H), 7.46 (d, $J = 4$ Hz, 1H), 7.01 (m, 2H), 3.78 (s, 3H), 2.85 (d, $J = 4$ Hz, 3H), 2.43 (m, 1H), 2.21 (s, 3H), 1.82 (m, 4 H), 1.71 (m, 1H), 1.35 (m, 4H), 1.26 (m, 1H); isomer 2, δ 9.35 (s, 1H), 8.71 (s, 1H), 8.35 (m, 1H), 8.23 (m, 1H), 7.76 (s, 1H), 7.65 (m, 1H), 7.55 (m, 1H), 7.44 (d, $J = 4$ Hz, 1H), 7.01 (m, 2H), 3.78 (s, 3H), 2.88 (d, $J = 4$ Hz, 3H), 2.43 (m, 1H), 2.17 (s, 3H), 1.82 (m, 4 H), 1.71 (m, 1H), 1.35 (m, 4H), 1.26 (m, 1H). Anal. ($\text{C}_{30}\text{H}_{32}\text{N}_6\text{O}_3 \cdot 0.33\text{H}_2\text{O}$) H, N, C: calcd 68.68, found 67.91.

2-Chloro-2'-fluoro-[3,4']bipyridinyl (27). To 2-fluoro-4-iodopyridine (**25**) (9.45 g, 42.4 mmol), 2-chloropyridine-3-boronic acid (**26**) (10.0 g, 63.5 mmol), Na_2CO_3 (13.5 g, 127 mmol), Pd(OAc) $_2$ (480 mg, 2.12 mmol), and P(tBu) $_3$ ·HBF $_4$ (1.23 g, 4.24 mmol) were added dioxane (125 mL) and water (45 mL). The mixture was heated overnight at 100 °C in a sealed tube. The resulting mixture was diluted with EtOAc and extracted with water and brine. The organic layer was dried over Na_2SO_4 , filtered, and concentrated. The resulting solid was triturated with hexanes and dried to yield the desired product as a tan solid (8.5 g, 96%): ^1H NMR (300 MHz, DMSO- d_6) δ 8.54 (dd, $J = 1.8, 4.5$ Hz, 1H), 8.38 (d, $J = 5.1$ Hz, 1H), 8.01 (dd, $J = 1.8, 7.5$ Hz, 1H), 7.60 (dd, $J = 4.5, 7.5$ Hz, 1H), 7.54 (m, 1H), 7.42 (m, 1H).

(2-Chloro-[3,4']bipyridinyl-2'-yl)methylamine (28). To 2-chloro-2'-fluoro-[3,4']bipyridinyl (**27**) (5.30 g, 25.4 mmol), *N*-methylamine hydrochloride (9.00 g, 133 mmol), and K_2CO_3 (28.1 g, 203 mmol) was added DMSO (70 mL). The mixture was heated overnight at 80 °C in a sealed tube. The cooled mixture was diluted with water (300 mL) and the resulting solid was filtered, washed with water, and dried to yield 4.96 g (89%) of product as a white solid: ^1H NMR (400 MHz, DMSO- d_6) δ 8.46 (d, $J = 3.2$ Hz, 1H), 8.06 (d, $J = 5.2$ Hz, 1H), 7.86 (dd, $J = 2, 7.6$ Hz, 1H), 7.53 (dd, $J = 4.8, 7.6$ Hz, 1H), 6.65 (m, 1H), 6.55 (dd, $J = 1.6, 5.2$ Hz, 1H), 6.47 (m, 1H), 2.79 (d, $J = 4.8$ Hz, 3H).

4-(2-Fluoropyridin-3-yl)quinoline (31). To 4-chloroquinoline (**29**) (245 mg, 1.50 mmol), 2-fluoropyridine-3-boronic acid (**30**) (232 mg, 1.65 mmol), and Pd(PPh $_3$) $_4$ (87 mg, 0.08 mmol) were added DME (4.0 mL) and 1 M NaHCO_3 (1.0 mL). The resulting mixture was heated to 80 °C for 20 h, diluted with EtOAc, and extracted with saturated Na_2CO_3 , water, and brine. The separated organic layer was dried over Na_2SO_4 , filtered, and concentrated. The resulting residue was purified by silica gel chromatography (25%–50% EtOAc/hexanes) to yield the desired product (282 mg, 60%): ^1H NMR (400 MHz, DMSO- d_6) δ 9.02 (d, $J = 4.4$ Hz, 1H), 8.46 (m, 1H), 8.17 (m, 1H), 8.15 (d, $J = 7.6$ Hz, 1H), 7.84 (m, 1H), 7.61 (m, 4H).

4-(2-Fluoropyridin-3-yl)-6,7-dimethoxyquinazoline (32). Following the procedure described for **31**, 4-chloro-6,7-dimethoxyquinazoline (**32**) (250 mg, 1.11 mmol) and 2-fluoropyridine-3-boronic acid (**30**) (263 mg, 1.86 mmol) provided the title compound (258 mg, 81%): ^1H NMR (400 MHz, DMSO- d_6) δ 9.19 (s, 1H), 8.50 (m, 1H), 8.30 (m, 1H), 7.63 (m, 1H), 7.84 (s, 1H), 6.96 (d, $J = 2.0$ Hz, 1H), 4.02 (s, 3H), 3.81 (s, 3H).

4-(2-Phenylamino)pyridin-3-yl)-N-(3,4,5-trimethoxyphenyl)-1,3,5-triazin-2-amine (34). Step 1. Triazine **20** (1.71 g, 7.54 mmol) and 3,4,5-trimethoxyaniline (1.5 g, 8.3 mmol) were stirred at room temperature for 1 day in 2-propanol (200 mL). NEt_3 (2 mL) was added and stirring was continued for a second day. The mixture was concentrated and the resulting solid triturated with *tert*-butyl methyl ether, which resulting in 2.5 g (89%) of product: ^1H NMR (300 MHz, DMSO- d_6) δ 10.23 (s, 1H), 8.71 (s, 1H), 8.39 (dd, $J = 3, 5$ Hz, 1H), 8.08 (br s, 1H), 7.43 (dd, $J = 5, 8$ Hz, 1H), 7.01 (s, 2H), 3.57 (s, 6H), 3.45 (s, 3H).

Step 2. 4-(2-Chloropyridin-3-yl)-*N*-(3,4,5-trimethoxyphenyl)-1,3,5-triazin-2-amine (25 mg, 0.07 mmol) was added to aniline (0.25 mL). The mixture was heated to 90 °C overnight. After cooling, the resulting solid was triturated with 2-propanol and filtered to produce 19 mg (68%) of the desired product: ^1H NMR (400 MHz,

DMSO- d_6) δ 11.62 (br s, 1H), 10.38 (s, 1H), 8.90 (s, 1H), 8.83 (dd, $J = 4, 8$ Hz, 1H), 8.39 (m, 1H), 7.82 (br s, 1H), 7.48 (br s, 1H), 7.25 (br s, 1H), 7.07 (m, 3H), 6.96 (m, 2H), 3.75 (s, 6H), 3.66 (s, 3H); HPLC purity = 99% (system A), 98% (system B); HRMS ($\text{C}_{23}\text{H}_{22}\text{N}_6\text{O}_3$) $^+$ calcd 431.18262, found 431.18335.

***N*-(4-Phenoxyphenyl)-2-(pyridin-4-ylmethylamino)nicotinamide (35).**²⁴ The compound was synthesized and purified according to procedures in ref 24. ^1H NMR (400 MHz, DMSO- d_6) δ 10.59 (s, 1H), 8.82 (m, 3H), 8.26 (m, 1H), 8.13 (m, 1H), 7.97 (m, 2H), 7.78 (d, $J = 8$ Hz, 2H), 7.40 (m, 2H), 7.15 (m, 1H), 7.06 (d, $J = 8$ Hz, 2H), 7.00 (d, $J = 8$ Hz, 2H), 6.82 (m, 1H), 5.00 (s, 2H). Anal. ($\text{C}_{24}\text{H}_{20}\text{N}_4\text{O}_2 \cdot 3\text{HCl}$) H, N, C: calcd 55.05, found 56.03.

***N*-(4-Phenoxyphenyl)-3-(3-(4-(3,4,5-trimethoxyphenylamino)-1,3,5-triazin-2-yl)pyridin-2-ylamino)benzamide (36).** 4-(2-chloropyridin-3-yl)-*N*-(3,4,5-trimethoxyphenyl)-1,3,5-triazin-2-amine (103 mg, 0.276 mmol) and 3-amino-*N*-(4-phenoxyphenyl)benzamide (297 mg, 0.976 mmol) were combined in DMSO (0.15 mL) and heated to 90 °C overnight. The mixture was cooled and the resulting slurry was triturated with 2-propanol and methanol before filtering to yield 153 mg (86%) of the product as a yellow solid: ^1H NMR (400 MHz, DMSO- d_6) δ 11.75 (br s, 1H), 10.42 (s, 1H), 10.25 (s, 1H), 8.96 (s, 1H), 8.84 (m, 1H), 8.42 (s, 1H), 8.25 (m, 1H), 8.08 (br s, 1H), 7.82 (d, $J = 8$ Hz, 2H), 7.60 (m, 2H), 7.45 (m, 2H), 7.13 (m, 3H), 7.03 (m, 5H), 3.76 (s, 6H), 3.64 (s, 3H); HPLC purity = 97% (system A), 96% (system B); HRMS ($\text{C}_{36}\text{H}_{31}\text{N}_7\text{O}_5$) $^+$ calcd 642.24594, found 642.24648.

4-Methyl-*N*-phenyl-3-(3-(pyrimidin-4-yl)pyridin-2-ylamino)benzamide (37). Following the procedure described for **6**, aniline and **12** provided the title compound (87 mg, 70%) as a yellow solid: ^1H NMR (400 MHz, DMSO- d_6) δ 11.68 (s, 1H), 10.18 (s, 1H), 9.39 (s, 1H), 8.89 (d, $J = 5$ Hz, 1H), 8.77 (s, 1H), 8.45 (d, $J = 7$ Hz, 1H), 8.32 (m, 1H), 8.26 (m, 1H), 7.75 (m, 2H), 7.55 (m, 1H), 7.37 (m, 1H), 7.31 (m, 2H), 7.05 (m, 1H), 6.95 (m, 1H), 2.48 (s, 3H); HPLC purity = 95% (system A), 95% (system B); HRMS ($\text{C}_{23}\text{H}_{19}\text{N}_5\text{O}$) $^+$ calcd 382.16624, found 382.16739.

4-Methyl-3-(3-(pyrimidin-4-yl)pyridin-2-ylamino)-*N*-(4-(trifluoromethyl)phenyl)benzamide (38). Following the procedure described for **6**, 4-trifluoromethylaniline and **12** provided the title compound (98 mg, 64%) as a yellow solid: mp = 268–270 °C; ^1H NMR (400 MHz, DMSO- d_6) δ 11.58 (s, 1H), 10.34 (s, 1H), 9.23 (s, 1H), 8.78 (d, $J = 4.7$ Hz, 1H), 8.66 (s, 1H), 8.35 (d, $J = 6.8$ Hz, 1H), 8.21 (m, 1H), 8.13 (m, 1H), 7.86 (d, $J = 7.8$ Hz, 1H), 7.55 (d, $J = 8.2$ Hz, 1H), 7.44 (d, $J = 7.4$ Hz, 1H), 7.27 (d, $J = 7.2$ Hz, 1H), 6.84 (m, 1H), 2.31 (s, 3H). Anal. ($\text{C}_{24}\text{H}_{18}\text{F}_3\text{N}_5\text{O} \cdot 0.33\text{H}_2\text{O}$) H, N, C: calcd 63.29, found 63.93.

***N*-(3-(3-(Dimethylamino)propyl)-5-(trifluoromethyl)phenyl)-4-methyl-3-(3-(pyrimidin-4-yl)pyridin-2-ylamino)benzamide (39).** Following the procedure described for **6**, 3-(3-(dimethylamino)propyl)-5-(trifluoromethyl)benzenamine and **12** provided the title compound (15 mg, 4%) as a yellow solid: ^1H NMR (400 MHz, DMSO- d_6) δ 11.73 (s, 1H), 10.38 (s, 1H), 9.38 (s, 1H), 8.93 (d, $J = 5$ Hz, 1H), 8.82 (s, 1H), 8.49 (d, $J = 8$ Hz, 1H), 8.37 (m, 1H), 8.2 (d, $J = 5$ Hz, 1H), 8.04 (s, 1H), 7.91 (s, 1H), 7.59 (d, $J = 5$ Hz, 1H), 7.42 (d, $J = 5$ Hz, 1H), 7.24 (s, 1H), 6.97 (m, 1H), 2.67 (m, 2H), 2.48 (s, 3H), 2.39 (m, 2H), 2.24 (s, 6H), 1.78 (m, 2H); HPLC purity = 97% (system A), 98% (system B); HRMS ($\text{C}_{29}\text{H}_{29}\text{F}_3\text{N}_6\text{O}$) $^+$ calcd 535.24277, found 535.24421.

4-Methyl-*N*-(2-(piperidin-1-yl)-5-(trifluoromethyl)phenyl)-3-(3-(pyrimidin-4-yl)pyridin-2-ylamino)benzamide (41). Following the procedure described for **6**, 2-(piperidin-1-yl)-5-(trifluoromethyl)benzenamine and **12** provided the title compound (12 mg, 7%) as a yellow solid: ^1H NMR (400 MHz, CDCl_3): δ 11.63 (s, 1H), 9.42 (br s, 1H), 9.26 (s, 1H), 8.81 (m, 2H), 8.39 (s, 1H), 8.17 (d, $J = 4.4$ Hz, 1H), 7.82 (s, 1H), 7.58 (m, 1H), 7.39 (d, $J = 4.4$ Hz, 1H), 7.33 (m, 1H), 7.21 (m, 1H), 6.88 (m, 1H), 2.83 (m, 4H), 2.52 (s, 3H), 1.71 (m, 4H), 1.58 (m, 2H); HPLC purity = 99% (system A), 99% (system B); HRMS ($\text{C}_{29}\text{H}_{27}\text{F}_3\text{N}_6\text{O}$) $^+$ calcd 533.22712, found 533.22866.

4-Methyl-3-(3-(pyrimidin-4-yl)pyridin-2-yloxy)-*N*-(3-(trifluoromethyl)phenyl)benzamide (42). Following the procedure described for **15**, 4-methyl-3-(3-(pyrimidin-4-yl)pyridin-2-yloxy)-

benzoic acid and 3-trifluoromethylaniline provided the title compound (61 mg, 41%) as a white solid: $^1\text{H NMR}$ (400 MHz, $\text{DMSO}-d_6$) δ 10.43 (s, 1H), 9.33 (d, $J = 1.2$ Hz, 1H), 8.91 (d, $J = 5.4$ Hz, 1H), 8.54 (dd, $J = 2.0, 7.4$ Hz, 1H), 8.28 (dd, $J = 1.6, 5.4$ Hz, 1H), 8.22 (dd, $J = 1.9, 4.6$ Hz, 1H), 8.18 (s, 1H), 8.02 (d, $J = 8.5$ Hz, 1H), 7.82 (d, $J = 7.8$ Hz, 1H), 7.78 (d, $J = 1.9$ Hz, 1H), 7.56 (m, 1H), 7.50 (d, $J = 8.2$ Hz, 1H), 7.42 (d, $J = 7.8$ Hz, 1H), 7.33 (dd, $J = 4.5, 7.5$ Hz, 1H), 2.18 (s, 3H). Anal. ($\text{C}_{24}\text{H}_{17}\text{F}_3\text{N}_4\text{O}_2 \cdot 0.33\text{H}_2\text{O}$) H, N, C: calcd 64.00, found 63.16.

4-Methyl-3-(3-(pyrimidin-4-yl)pyridin-2-yloxy)-*N*-(4-(trifluoromethyl)phenyl)benzamide (43). Following the procedure described for **15**, 4-methyl-3-(3-(pyrimidin-4-yl)pyridin-2-yloxy)benzoic acid and 4-trifluoromethylaniline provided the title compound as a white solid: mp = 190–193 °C; $^1\text{H NMR}$ (400 MHz, $\text{DMSO}-d_6$) δ 10.45 (s, 1H), 9.37 (s, 1H), 8.96 (d, $J = 4$ Hz, 1H), 8.57 (dd, $J = 4, 8$ Hz, 1H), 8.32 (dd, $J = 2, 4$ Hz, 1H), 8.26 (dd, $J = 2, 4$ Hz, 1H), 8.00 (d, $J = 8$ Hz, 2H), 7.86 (dd, $J = 2, 8$ Hz, 1H), 7.82 (d, $J = 8$ Hz, 1H), 7.72 (d, $J = 8$ Hz, 2H), 7.53 (d, $J = 8$ Hz, 1H), 7.37 (dd, $J = 4, 8$ Hz, 1H), 2.20 (s, 3H); HPLC purity = 98% (system A), 97% (system C); HRMS ($\text{C}_{24}\text{H}_{17}\text{F}_3\text{N}_4\text{O}_2$) $^+$ calcd 451.13764, found 451.13711.

***N*-(2-Methoxy-5-(trifluoromethyl)phenyl)-4-methyl-3-(3-(pyrimidin-4-yl)pyridin-2-yloxy)benzamide (44).** Following the procedure described for **15**, 4-methyl-3-(3-(pyrimidin-4-yl)pyridin-2-yloxy)benzoic acid and 2-methoxy-5-(trifluoromethyl)benzenamine provided the title compound (30 mg, 39%) as a white solid: $^1\text{H NMR}$ (400 MHz, CDCl_3): δ 9.39 (s, 1H), 8.84 (d, $J = 1$ Hz, 1H), 8.82 (d, $J = 4$ Hz, 1H), 8.67 (d, $J = 8$ Hz, 1H), 8.58 (s, 1H), 8.25 (d, $J = 4$ Hz, 1H), 8.22 (m, 1H), 7.67 (m, 2H), 7.43 (d, $J = 8$ Hz, 1H), 7.38 (d, $J = 8$ Hz, 1H), 7.22 (m, 1H), 6.96 (d, $J = 8$ Hz, 1H), 3.97 (s, 3H), 2.25 (s, 3H). Anal. ($\text{C}_{25}\text{H}_{19}\text{F}_3\text{N}_4\text{O}_3 \cdot 0.33\text{H}_2\text{O}$) H, N, C: calcd 61.73, found 62.39.

4-Methyl-*N*-(2-(piperidin-1-yl)-5-(trifluoromethyl)phenyl)-3-(3-(pyrimidin-4-yl)pyridin-2-yloxy)benzamide (45). Following the procedure described for **15**, 4-methyl-3-(3-(pyrimidin-4-yl)pyridin-2-yloxy)benzoic acid and 2-(piperidin-1-yl)-5-(trifluoromethyl)benzenamine provided the title compound (42 mg, 58%) as a white solid: $^1\text{H NMR}$ (400 MHz, $\text{DMSO}-d_6$) δ 9.53 (s, 1H), 9.37 (s, 1H), 8.94 (d, $J = 8$ Hz, 1H), 8.59 (dd, $J = 4, 8$ Hz, 1H), 8.39 (d, $J = 2$ Hz, 1H), 8.28 (m, 2H), 7.81 (d, $J = 4$ Hz, 1H), 7.71 (s, 1H), 7.57 (d, $J = 8$ Hz, 1H), 7.49 (m, 1H), 7.40 (m, 2H), 2.84 (m, 4H), 2.25 (s, 3H), 1.53 (m, 4H), 1.45 (m, 2H). Anal. ($\text{C}_{29}\text{H}_{26}\text{F}_3\text{N}_5\text{O}_2 \cdot 0.5\text{H}_2\text{O}$) H, N, C: calcd 64.20, found 64.90.

4-Methyl-*N*-(2-morpholino-5-(trifluoromethyl)phenyl)-3-(3-(pyrimidin-4-yl)pyridin-2-yloxy)benzamide (46). Following the procedure described for **15**, 4-methyl-3-(3-(pyrimidin-4-yl)pyridin-2-yloxy)benzoic acid and 3-amino-4-(4-morpholino)benzotrifluoride provided the title compound (49 mg, 54%) as a white solid: $^1\text{H NMR}$ (400 MHz, $\text{DMSO}-d_6$) δ 9.67 (s, 1H), 9.37 (s, 1H), 8.95 (d, $J = 4$ Hz, 1H), 8.28 (m, 2H), 7.81 (d, $J = 4$ Hz, 1H), 7.77 (s, 1H), 7.53 (d, $J = 4$ Hz, 1H), 7.51 (m, 1H), 7.38 (m, 2H), 3.68 (m, 4H), 2.91 (m, 4H), 2.33 (s, 3H). Anal. ($\text{C}_{28}\text{H}_{24}\text{F}_3\text{N}_5\text{O}_3 \cdot 0.5\text{H}_2\text{O}$) H, N, C: calcd 61.76, found 62.47.

4-Methyl-3-(3-(2-(methylamino)pyrimidin-4-yl)pyridin-2-yloxy)-*N*-(2-morpholino-5-(trifluoromethyl)phenyl)benzamide (47). Following the procedure described for **15**, **14** and 3-amino-4-(4-morpholino)benzotrifluoride provided the title compound (28 mg, 28%) as a white solid: $^1\text{H NMR}$ (400 MHz, CDCl_3): δ 9.37 (s, 1H), 8.89 (s, 1H), 8.60 (br s, 1H), 8.38 (d, $J = 2$ Hz, 1H), 8.22 (d, $J = 2$ Hz, 1H), 7.66 (m, 2H), 7.47 (m, 2H), 7.38 (d, $J = 4$ Hz, 1H), 7.25 (d, $J = 4$ Hz, 1H), 7.19 (m, 1H), 5.44 (br s, 1H), 3.80 (m, 4H), 3.11 (d, $J = 4$ Hz, 3H), 2.91 (m, 4H), 2.29 (s, 3H). Anal. ($\text{C}_{29}\text{H}_{27}\text{F}_3\text{N}_6\text{O}_3 \cdot 0.5\text{H}_2\text{O}$) C, H, N.

***N*-(5-Cyclohexyl-2-methoxyphenyl)-4-methyl-3-(3-(2-(methylamino)pyrimidin-4-yl)pyridin-2-yloxy)benzamide (48).** Following the procedure described for **15**, **14** and 5-cyclohexyl-2-methoxybenzenamine provided the title compound (37 mg, 64%) as an off-white solid: $^1\text{H NMR}$ (300 MHz, $\text{DMSO}-d_6$) δ 9.39 (s, 1H), 8.50 (br s, 1H), 8.38 (d, $J = 4.5$ Hz, 1H), 8.16 (m, 1H), 7.78 (m, 1H), 7.69 (m, 1H), 7.49 (m, 1H), 7.45 (d, $J = 7.6$ Hz, 1H), 7.31 (m, 2H), 7.22 (m, 1H), 6.99 (m, 2H), 3.76 (s, 3H), 2.87 (d,

$J = 4.5$ Hz, 3H), 2.42 (m, 1H), 2.17 (s, 3H), 1.77 (m, 4H), 1.64 (m, 1H), 1.35 (m, 4H), 1.24 (m, 1H). Anal. ($\text{C}_{31}\text{H}_{33}\text{N}_5\text{O}_3$) H, N, C: calcd 71.11, found 70.60.

***N*-(5-Cyclohexyl-2-methoxyphenyl)-4-methyl-3-(3-(2-(methylamino)pyridin-4-yl)pyridin-2-yloxy)benzamide (49).** Following the procedure described for **24**, **28** and *N*-(5-cyclohexyl-2-methoxyphenyl)-3-hydroxy-4-methylbenzamide provided the title compound (82 mg, 60%): $^1\text{H NMR}$ (400 MHz, $\text{DMSO}-d_6$) δ 9.39 (s, 1H), 8.09 (dd, $J = 1.7, 4.8$ Hz, 1H), 8.05 (d, $J = 5.1$ Hz, 1H), 7.94 (dd, $J = 1.4, 7.5$ Hz, 1H), 7.73 (d, $J = 8.2$ Hz, 1H), 7.64 (s, 1H), 7.48 (m, 1H), 7.42 (d, $J = 7.9$ Hz, 1H), 7.23 (dd, $J = 5.1, 7.5$ Hz, 1H), 6.98 (m, 2H), 6.79 (d, $J = 5.5$ Hz, 1H), 6.76 (s, 1H), 6.63 (m, 1H), 3.74 (s, 3H), 2.77 (d, $J = 4.5$ Hz, 3H), 2.42 (m, 1H), 2.14 (s, 3H), 1.74 (m, 4H), 1.66 (m, 1H), 1.32 (m, 4H), 1.19 (m, 1H). Anal. ($\text{C}_{32}\text{H}_{34}\text{N}_4\text{O}_3 \cdot 0.33\text{H}_2\text{O}$) C, H, N.

***N*-(5-Cyclohexyl-2-methoxyphenyl)-4-methyl-3-(3-(quinolin-4-yl)pyridin-2-yloxy)benzamide (50).** Following the procedure described for **24**, **31** and *N*-(5-cyclohexyl-2-methoxyphenyl)-3-hydroxy-4-methylbenzamide provided the title compound (41 mg, 57%): $^1\text{H NMR}$ (300 MHz, $\text{DMSO}-d_6$) δ 9.36 (s, 1H), 9.01 (d, $J = 4.5$ Hz, 1H), 8.27 (m, 1H), 8.16 (d, $J = 7.6$ Hz, 1H), 7.97 (m, 1H), 7.77 (m, 2H), 7.63 (m, 4H), 7.49 (m, 1H), 7.36 (m, 1H), 7.34 (d, $J = 7.5$ Hz, 1H), 6.97 (m, 2H), 3.76 (s, 3H), 2.45 (m, 1H), 2.00 (s, 3H), 1.77 (m, 4H), 1.68 (m, 1H), 1.35 (m, 4H), 1.21 (m, 1H). Anal. ($\text{C}_{35}\text{H}_{33}\text{N}_5\text{O}_3 \cdot 0.5\text{H}_2\text{O}$) C, H, N.

***N*-(5-Cyclohexyl-2-methoxyphenyl)-3-(3-(6,7-dimethoxyquinolin-4-yl)pyridin-2-yloxy)-4-methylbenzamide (51).** Following the procedure described for **24**, **33** and *N*-(5-cyclohexyl-2-methoxyphenyl)-3-hydroxy-4-methylbenzamide provided the title compound (29 mg, 35%): $^1\text{H NMR}$ (400 MHz, $\text{DMSO}-d_6$) δ 9.40 (s, 1H), 9.20 (s, 1H), 8.37 (m, 1H), 8.10 (d, $J = 7$ Hz, 1H), 7.71 (d, $J = 7.6$ Hz, 1H), 7.65 (s, 1H), 7.60 (m, 2H), 7.48 (m, 2H), 7.39 (m, 1H), 7.28 (d, $J = 7.6$ Hz, 1H), 7.05 (s, 1H), 6.98 (m, 2H), 4.01 (s, 3H), 3.82 (s, 3H), 3.76 (s, 3H), 2.45 (m, 1H), 2.00 (s, 3H), 1.77 (m, 4H), 1.68 (m, 1H), 1.35 (m, 4H), 1.21 (m, 1H). Anal. ($\text{C}_{36}\text{H}_{36}\text{N}_4\text{O}_5 \cdot 0.33\text{H}_2\text{O}$) H, N, C: calcd 71.51, found 70.80.

4-Methyl-3-(3-(2-(methylamino)pyrimidin-4-yl)pyridin-2-yloxy)-*N*-(2-(piperidin-1-yl)-5-(trifluoromethyl)phenyl)benzamide (55). Following the procedure described for **15**, **14** and 2-(piperidin-1-yl)-5-(trifluoromethyl)benzenamine provided the title compound (19 mg, 31%): $^1\text{H NMR}$ (300 MHz, $\text{DMSO}-d_6$) δ 9.53 (s, 1H), 8.50 (br s, 1H), 8.35 (m, 1H), 8.19 (m, 1H), 7.75 (m, 1H), 7.63 (m, 1H), 7.54 (d, $J = 8.4$ Hz, 1H), 7.42 (m, 1H), 7.32 (m, 2H), 7.21 (m, 1H), 2.87 (d, $J = 4.8$ Hz, 3H), 2.82 (m, 4H), 2.23 (s, 3H), 1.53 (m, 4H), 1.42 (m, 2H); HPLC purity = 95% (system A), 96% (system B); HRMS ($\text{C}_{30}\text{H}_{29}\text{F}_3\text{N}_6\text{O}_2$) $^+$ calcd 563.23769, found 563.23706.

2-Fluoro-5-(3-(2-(methylamino)pyrimidin-4-yl)pyridin-2-yloxy)-*N*-(2-(piperidin-1-yl)-5-(trifluoromethyl)phenyl)benzamide (57). Following the procedure described for **15**, 2-fluoro-5-(3-(2-(methylamino)pyrimidin-4-yl)pyridin-2-yloxy)benzoic acid and 2-(piperidin-1-yl)-5-(trifluoromethyl)benzenamine provided the title compound (290 mg, 67%): $^1\text{H NMR}$ (400 MHz, $\text{DMSO}-d_6$) δ 9.95 (d, $J = 9$ Hz, 1H), 8.67 (s, 1H), 8.48 (br s, 1H), 8.39 (d, $J = 4$ Hz, 1H), 8.24 (m, 1H), 7.75 (m, 1H), 7.55 (m, 4H), 7.36 (dd, $J = 2, 4$ Hz, 1H), 7.30 (d, $J = 4$ Hz, 1H), 7.20 (m, 1H), 2.87 (m, 7 H), 1.70 (m, 4H), 1.57 (m, 2H). Anal. ($\text{C}_{29}\text{H}_{26}\text{F}_4\text{N}_6\text{O}_2 \cdot 0.33\text{H}_2\text{O}$) H, N, C: calcd 61.48, found 60.84.

***N*-(2-((3-(Dimethylamino)propyl)(methylamino)-5-(trifluoromethyl)phenyl)-2-fluoro-5-(3-(2-(methylamino)pyrimidin-4-yl)pyridin-2-yloxy)benzamide (58).** Following the procedure described for **15**, 2-fluoro-5-(3-(2-(methylamino)pyrimidin-4-yl)pyridin-2-yloxy)benzoic acid and *N*-(3-(dimethylamino)propyl)-*N*-(methyl-4-(trifluoromethyl)benzene)-1,2-diamine provided the title compound (143 mg, 54%): $^1\text{H NMR}$ (400 MHz, $\text{DMSO}-d_6$) δ 10.50 (br s, 1H), 9.94 (d, $J = 9.5$ Hz, 1H), 8.52 (s, 1H), 8.39 (d, $J = 3.7$ Hz, 1H), 8.24 (d, $J = 6.6$ Hz, 1H), 7.74 (d, $J = 5.2$ Hz, 1H), 7.50 (m, 4H), 7.35 (m, 1H), 7.29 (d, $J = 4.4$ Hz, 1H), 7.24 (d, $J = 4.4$ Hz, 1H), 3.05 (m, 2H), 2.98 (m, 2H), 2.87 (d, $J = 4.4$ Hz, 3H), 2.69 (s, 3H), 2.62 (s, 6H), 1.86 (m, 2H). Anal. ($\text{C}_{30}\text{H}_{31}\text{F}_4\text{N}_7\text{O}_2 \cdot 0.33\text{H}_2\text{O}$) H, N, C: calcd 60.29, found 59.69.

4-Methyl-3-(3-(4-(methylamino)-1,3,5-triazin-2-yl)pyridin-2-yloxy)-*N*-(2-(piperidin-1-yl)-5-(trifluoromethyl)phenyl)benzamide (60). Following the procedure described for **15**, 4-methyl-3-(3-(4-(methylamino)-1,3,5-triazin-2-yl)pyridin-2-yloxy)benzoic acid and 2-(piperidin-1-yl)-5-(trifluoromethyl)benzenamine provided the title compound (51 mg, 40%): ¹H NMR (400 MHz, two inseparable isomers present in DMSO-*d*₆) isomer 1, δ 9.52 (s, 1H), 8.68 (s, 1H), 8.37 (m, 1H), 8.24 (m, 1H), 8.08 (m, 1H), 7.72 (d, *J* = 7.8 Hz, 1H), 7.56 (d, *J* = 7.5 Hz, 1H), 7.50 (d, *J* = 7.5 Hz, 1H), 7.44 (d, *J* = 8.5 Hz, 1H), 7.33 (d, *J* = 8.2 Hz, 1H), 7.29 (m, 1H), 2.85 (d, *J* = 4.8 Hz, 3H), 2.79 (m, 4H), 2.20 (s, 3H), 1.50 (m, 4H), 1.41 (m, 2H); isomer 2, δ 9.50 (s, 1H), 8.58 (s, 1H), 8.37 (m, 1H), 8.24 (m, 1H), 8.08 (m, 1H), 7.72 (d, *J* = 7.8 Hz, 1H), 7.56 (d, *J* = 7.5 Hz, 1H), 7.50 (d, *J* = 7.5 Hz, 1H), 7.44 (d, *J* = 8.5 Hz, 1H), 7.33 (d, *J* = 8.2 Hz, 1H), 7.29 (m, 1H), 2.79 (m, 4H), 2.78 (d, *J* = 4.8 Hz, 3H), 2.23 (s, 3H), 1.50 (m, 4H), 1.41 (m, 2H). Anal. (C₂₉H₂₈F₃N₇O₂·0.33H₂O) H, N, C: calcd 61.80, found 61.15.

***N*-(2-((3-(Dimethylamino)propyl)(methylamino)-5-(trifluoromethyl)phenyl)-4-methyl-3-(3-(4-(methylamino)-1,3,5-triazin-2-yl)pyridin-2-yloxy)benzamide (61).** Following the procedure described for **15**, 4-methyl-3-(3-(4-(methylamino)-1,3,5-triazin-2-yl)pyridin-2-yloxy)benzoic acid and *N*¹-(3-(dimethylamino)propyl)-*N*¹-methyl-4-(trifluoromethyl)benzene-1,2-diamine provided the title compound (87 mg, 27%): ¹H NMR (400 MHz, two inseparable isomers present in CDCl₃) isomer 1, δ 9.25 (s, 1H), 8.81 (m, 1H), 8.62 (s, 1H), 8.40 (dd, *J* = 2, 8 Hz, 1H), 8.26 (m, 1H), 7.66 (m, 2H), 7.43 (m, 1H), 7.34 (m, 1H), 7.28 (m, 1H), 7.16 (m, 1H), 3.03 (d, *J* = 8 Hz, 3H), 2.71 (s, 3H), 2.63 (m, 2H), 2.43 (br s, 6H), 2.32 (s, 3H), 1.85 (m, 2H), 1.04 (m, 2H); isomer 2, δ 9.25 (s, 1H), 8.81 (m, 1H), 8.75 (s, 1H), 8.22 (dd, *J* = 2, 8 Hz, 1H), 8.26 (m, 1H), 7.66 (m, 2H), 7.43 (m, 1H), 7.34 (m, 1H), 7.28 (m, 1H), 7.16 (m, 1H), 3.09 (d, *J* = 8 Hz, 3H), 2.71 (s, 3H), 2.63 (m, 2H), 2.43 (br s, 6H), 2.24 (s, 3H), 1.85 (m, 2H), 1.04 (m, 2H). Anal. (C₃₀H₃₃F₃N₈O₂·0.33H₂O) H, N, C: calcd 60.60, found 59.99.

2-Fluoro-5-(3-(4-(methylamino)-1,3,5-triazin-2-yl)pyridin-2-yloxy)-*N*-(2-(piperidin-1-yl)-5-(trifluoromethyl)phenyl)benzamide (62). Following the procedure described for **15**, 2-fluoro-3-(3-(4-(methylamino)-1,3,5-triazin-2-yl)pyridin-2-yloxy)benzoic acid and 2-(piperidin-1-yl)-5-(trifluoromethyl)benzenamine provided the title compound (10 mg, 7%): ¹H NMR (400 MHz, two inseparable isomers present in CDCl₃) isomer 1, δ 10.05 (d, *J* = 9 Hz, 1H), 8.91 (m, 1H), 8.77 (s, 1H), 8.42 (dd, *J* = 2, 8 Hz, 1H), 8.27 (m, 1H), 8.01 (m, 1H), 7.42 (m, 1H), 7.36 (m, 1H), 7.27 (m, 1H), 7.18 (m, 1H), 3.08 (d, *J* = 8 Hz, 3H), 2.84 (m, 4H), 1.77 (m, 4H), 1.63 (m, 2H); isomer 2, δ 10.05 (d, *J* = 9 Hz, 1H), 8.91 (m, 1H), 8.63 (s, 1H), 8.27 (m, 2H), 8.01 (m, 1H), 7.42 (m, 1H), 7.36 (m, 1H), 7.27 (m, 1H), 7.18 (m, 1H), 3.04 (d, *J* = 8 Hz, 3H), 2.84 (m, 4H), 1.77 (m, 4H), 1.63 (m, 2H); HPLC purity = 96% (system A), 97% (system C); HRMS (C₃₀H₂₉F₃N₆O₂)⁺ calcd 563.23769, found 563.23706.

***N*-(2-((3-(Dimethylamino)propyl)(methylamino)-5-(trifluoromethyl)phenyl)-2-fluoro-5-(3-(4-(methylamino)-1,3,5-triazin-2-yl)pyridin-2-yloxy)benzamide (63).** Following the procedure described for **15**, 2-fluoro-5-(3-(4-(methylamino)-1,3,5-triazin-2-yl)pyridin-2-yloxy)benzoic acid and *N*¹-(3-(dimethylamino)propyl)-*N*¹-methyl-4-(trifluoromethyl)benzene-1,2-diamine provided the title compound (69 mg, 41%): ¹H NMR (300 MHz, two inseparable isomers present in DMSO-*d*₆) isomer 1, δ 9.97 (d, *J* = 6.9 Hz, 1H), 8.59 (s, 1H), 8.54 (m, 1H), 8.39 (d, *J* = 4 Hz, 1H), 8.27 (m, 2H), 8.14 (m, 1H), 7.62 (m, 1H), 7.49 (m, 4H), 7.36 (m, 1H), 2.99 (m, 2H), 2.79 (d, *J* = 3.3 Hz, 3H), 2.68 (s, 3H), 2.21 (m, 2H), 2.03 (s, 6H), 1.57 (m, 2H); isomer 2, δ 9.97 (d, *J* = 6.9 Hz, 1H), 8.69 (s, 1H), 8.54 (m, 1H), 8.27 (m, 3H), 8.14 (m, 1H), 7.62 (m, 1H), 7.49 (m, 4H), 7.36 (m, 1H), 2.99 (m, 2H), 2.86 (d, *J* = 3.3 Hz, 3H), 2.68 (s, 3H), 2.21 (m, 2H), 2.03 (s, 6H), 1.57 (m, 2H). Anal. (C₂₉H₃₀F₄N₈O₂·0.33H₂O) H, N, C: calcd 58.19, found 57.67.

***N*-(2-((3-(Dimethylamino)propyl)(methylamino)-5-isopropylphenyl)-2-fluoro-5-(3-(4-(methylamino)-1,3,5-triazin-2-yl)pyridin-2-yloxy)benzamide (64).** Following the procedure described for **15**, 2-fluoro-5-(3-(4-(methylamino)-1,3,5-triazin-2-yl)pyridin-2-yloxy)benzoic acid and *N*¹-(3-(dimethylamino)propyl)-4-isopro-

pyl-*N*¹-methylbenzene-1,2-diamine provided the title compound (167 mg, 66%): ¹H NMR (400 MHz, two inseparable isomers present in DMSO-*d*₆) isomer 1, δ 9.93 (d, *J* = 8 Hz, 1H), 8.59 (s, 1H), 8.49 (d, *J* = 2 Hz, 1H), 8.31 (m, 2H), 8.11 (m, 1H), 7.66 (m, 1H), 7.46 (m, 2H), 7.35 (m, 1H), 7.26 (d, *J* = 8 Hz, 1H), 7.03 (d, *J* = 4 Hz, 1H), 2.88 (m, 4H), 2.80 (m, 2H), 2.58 (s, 3H), 2.38 (m, 2H), 2.17 (s, 6H), 1.57 (m, 2H), 1.20 (d, *J* = 8 Hz, 6H); isomer 2, δ 9.93 (d, *J* = 8 Hz, 1H), 8.69 (s, 1H), 8.31 (m, 3H), 8.11 (m, 1H), 7.66 (m, 1H), 7.46 (m, 2H), 7.35 (m, 1H), 7.26 (d, *J* = 8 Hz, 1H), 7.03 (d, *J* = 4 Hz, 1H), 2.88 (m, 4H), 2.80 (m, 2H), 2.58 (s, 3H), 2.38 (m, 2H), 2.17 (s, 6H), 1.57 (m, 2H), 1.20 (d, *J* = 8 Hz, 6H). Anal. (C₃₁H₃₇FN₈O₂·0.33H₂O) H, N, C: calcd 65.02, found 64.34.

***N*-(5-Cyclopropyl-2-((3-(dimethylamino)propyl)(methylamino)phenyl)-2-fluoro-5-(3-(4-(methylamino)-1,3,5-triazin-2-yl)pyridin-2-yloxy)benzamide (65).** Following the procedure described for **15**, 2-fluoro-5-(3-(4-(methylamino)-1,3,5-triazin-2-yl)pyridin-2-yloxy)benzoic acid and 4-cyclopropyl-*N*¹-(3-(dimethylamino)propyl)-*N*¹-methylbenzene-1,2-diamine provided the title compound (97 mg, 35%): ¹H NMR (400 MHz, two inseparable isomers present in DMSO-*d*₆) isomer 1, δ 9.98 (d, *J* = 11.0 Hz, 1H), 8.69 (s, 1H), 8.40 (d, *J* = 7.4, 1H), 8.27 (m, 1H), 8.12 (br s, 2H), 7.65 (br s, 1H), 7.46 (m, 2H), 7.36 (m, 1H), 7.21 (d, *J* = 8.0 Hz, 1H), 6.86 (d, *J* = 8.0 Hz, 1H), 2.86 (d, *J* = 4.1 Hz, 3H), 2.84 (m, 2H), 2.55 (s, 3H), 2.17 (m, 2H), 1.99 (s, 6H), 1.88 (m, 1H), 1.48 (m, 2H), 0.91 (m, 2H), 0.61 (m, 2H); isomer 2, δ 9.98 (d, *J* = 11.0 Hz, 1H), 8.59 (s, 1H), 8.32 (d, *J* = 7.4, 1H), 8.27 (m, 1H), 8.12 (br s, 2H), 7.65 (br s, 1H), 7.46 (m, 2H), 7.36 (m, 1H), 7.21 (d, *J* = 8.0 Hz, 1H), 6.86 (d, *J* = 8.0 Hz, 1H), 2.84 (m, 2H), 2.79 (d, *J* = 4.8 Hz, 3H), 2.55 (s, 3H), 2.17 (m, 2H), 1.99 (s, 6H), 1.88 (m, 1H), 1.48 (m, 2H), 0.91 (m, 2H), 0.61 (m, 2H). Anal. (C₃₁H₃₅FN₈O₂·0.33H₂O) H, N, C: calcd 65.25, found 64.57.

4-Methyl-3-(3-(pyrimidin-4-yl)pyridin-2-yloxy)benzoic Acid. The title compound was synthesized following the procedure described for **14**: ¹H NMR (400 MHz, DMSO-*d*₆) δ 9.32 (d, *J* = 1.1 Hz, 1H), 8.89 (d, *J* = 5.4 Hz, 1H), 8.52 (dd, *J* = 1.9, 7.4 Hz, 1H), 8.26 (dd, *J* = 1.5, 5.4 Hz, 1H), 8.21 (dd, *J* = 2.0, 5.1 Hz, 1H), 7.73 (dd, *J* = 1.6, 7.8 Hz, 1H), 7.63 (d, *J* = 2.0 Hz, 1H), 7.43 (d, *J* = 7.8 Hz, 1H), 7.32 (dd, *J* = 5.0, 7.8 Hz, 1H).

2-Fluoro-5-hydroxybenzoic Acid. To 2-fluoro-5-methoxybenzoic acid (15.0 g, 88.2 mmol) were added HBr (150 mL, 49% aqueous) and glacial acetic acid (120 mL). A reflux condenser was attached and the mixture was heated to 140 °C for 16 h. After cooling the reaction to approximately 10 °C, the resulting solid was filtered, washed with water, and dried to yield 13.6 g (99%) of the title compound as a white solid: ¹H NMR (300 MHz, DMSO-*d*₆) δ 9.71 (s, 1H), 7.18 (m, 1H), 7.11 (m, 1H), 6.96 (m, 1H).

2-Fluoro-5-(3-(4-(methylamino)-1,3,5-triazin-2-yl)pyridin-2-yloxy)benzoic Acid. The title compound was synthesized following the procedure described for **14**: ¹H NMR (300 MHz, DMSO-*d*₆, two inseparable isomers present in DMSO) isomer 1, δ 8.67 (s, 1H), 8.34 (m, 1H), 8.24 (m, 1H), 8.10 (br s, 1H), 7.48 (m, 1H), 7.35 (m, 3H), 2.85 (d, *J* = 4.8 Hz, 3H); isomer 2, δ 8.56 (s, 1H), 8.24 (m, 2H), 8.10 (br s, 1H), 7.48 (m, 1H), 7.35 (m, 3H), 2.78 (d, *J* = 4.8 Hz, 3H).

***N*¹-(3-(Dimethylamino)propyl)-*N*¹-methyl-4-(trifluoromethyl)benzene-1,2-diamine. Step 1.** *N*¹,*N*¹,*N*³-Trimethylpropane-1,3-diamine (0.84 mL, 5.74 mmol) and sodium bicarbonate (1.1 g, 13 mmol) were added to 1-fluoro-2-nitro-4-(trifluoromethyl)benzene (1.0 g, 4.8 mmol) in THF (25 mL). The mixture was stirred at room temperature for 1 h, filtered, and concentrated. The crude material was dissolved in CH₂Cl₂ and extracted with water. The organic layer was dried over anhydrous sodium sulfate, filtered, and concentrated to yield 1.42 g (97%) of *N*-(3-(dimethylamino)propyl)-*N*-methyl-2-nitro-4-(trifluoromethyl)benzenamine as an orange oil: ¹H NMR (400 MHz, CDCl₃) δ 8.01 (s, 1H), 7.55 (dd, *J* = 2, 9 Hz, 1H), 7.16 (d, *J* = 9 Hz, 1H), 3.39 (m, 2H), 2.86 (s, 3H), 2.31 (m, 2H), 2.22 (s, 6H), 1.83 (m, 2H).

Step 2. *N*-(3-(Dimethylamino)propyl)-*N*-methyl-2-nitro-4-(trifluoromethyl)benzenamine (1.42 g, 4.65 mmol) was dissolved in MeOH (46 mL), and 10% Pd/C (0.493 g, 0.465 mmol) was added.

The reaction flask was purged with hydrogen before being stirred at room temperature under a hydrogen atmosphere for 20 h. The mixture was filtered through a pad of Celite and concentrated to yield 1.17 g (91%) of *N*¹-(3-(dimethylamino)propyl)-*N*¹-methyl-4-(trifluoromethyl)benzene-1,2-diamine as a red oil: ¹H NMR (400 MHz, CDCl₃): δ 7.25 (s, 1H), 7.02 (d, *J* = 8 Hz, 1H), 6.90 (m, 1H), 4.53 (br s, 2H), 2.87 (m, 2H), 2.64 (s, 3H), 2.37 (m, 2H), 2.20 (s, 6H), 1.69 (m, 2H).

***N*¹-(3-(Dimethylamino)propyl)-4-isopropyl-*N*¹-methylbenzene-1,2-diamine. Step 1.** 2-(Dicyclohexylphosphino)-2'-(*N,N*-dimethylamino)biphenyl (32 mg, 0.08 mmol), Pd₂(dba)₃ (19 mg, 0.02 mmol), and NaOtBu (0.55 g, 5.7 mmol) were added to an argon-purged reaction vessel containing dioxane (8 mL) and *t*BuOH (4 mL). 1-Iodo-4-isopropylbenzene (1.0 g, 4.1 mmol) and *N*¹,*N*¹,*N*³-trimethylpropane-1,3-diamine (0.71 mL, 4.9 mmol) were added and the mixture was heated to 60 °C for 24 h.³¹ The cooled reaction was diluted with Et₂O and filtered through a pad of Celite. The crude material was purified by silica gel chromatography (0–10% MeOH/CH₂Cl₂) to yield 830 mg (87%) of *N*-(3-(dimethylamino)propyl)-4-isopropyl-*N*-methylbenzenamine as an orangish oil: ¹H NMR (400 MHz, DMSO-*d*₆) δ 7.00 (d, *J* = 8 Hz, 2H), 6.61 (d, *J* = 8 Hz, 2H), 3.23 (m, 2H), 2.81 (s, 3H), 2.72 (sept, *J* = 4 Hz, 1H), 2.19 (m, 2H), 2.10 (s, 6H), 1.58 (m, 2H), 1.14 (d, *J* = 4 Hz, 6H).

Step 2. To a 0 °C solution of nitronium tetrafluoroborate (454 mg, 3.42 mmol) in CH₃CN (17 mL) was added dropwise over 10 min *N*-(3-(dimethylamino)propyl)-4-isopropyl-*N*-methylbenzenamine (400 mg, 1.71 mmol) in CH₃CN (17 mL).³² The mixture was stirred at room temperature for 18 h, concentrated, and purified by Gilson reverse-phase HPLC. After diluting with CH₂Cl₂ and neutralizing with saturated sodium carbonate, the organic layer was separated and dried over anhydrous sodium sulfate. This layer was filtered and concentrated to provide 300 mg (63%) of *N*-(3-(dimethylamino)propyl)-4-isopropyl-*N*-methyl-2-nitrobenzenamine as an orange oil: ¹H NMR (400 MHz, DMSO-*d*₆) δ 7.57 (d, *J* = 2 Hz, 1H), 7.42 (dd, *J* = 2, 8 Hz, 1H), 7.23 (d, *J* = 8 Hz, 1H), 3.08 (m, 2H), 2.88 (sept, *J* = 4 Hz, 1H), 2.67 (s, 3H), 2.61 (m, 2H), 2.43 (s, 6H), 1.72 (m, 2H), 1.17 (d, *J* = 4 Hz, 6H).

Step 3. To *N*-(3-(dimethylamino)propyl)-4-isopropyl-*N*-methyl-2-nitrobenzenamine (1.0 g, 3.6 mmol) in MeOH (36 mL) was added 10% Pd/C (190 mg, 0.18 mmol). Hydrogen gas was bubbled through the reaction before it was stirred at room temperature for 18 h under a hydrogen atmosphere. The reaction was filtered through a pad of Celite and purified by silica gel chromatography (90:10:1 CH₂Cl₂/MeOH/NH₄OH) to obtain 373 mg (42%) of *N*¹-(3-(dimethylamino)propyl)-4-isopropyl-*N*¹-methylbenzene-1,2-diamine as a brown oil: ¹H NMR (500 MHz, CDCl₃): δ 6.93 (d, *J* = 8 Hz, 1H), 6.58 (m, 1H), 6.57 (m, 1H), 3.80 (br s, 2H), 2.86 (m, 2H), 2.76 (sept, *J* = 4 Hz, 1H), 2.62 (s, 3H), 2.34 (m, 2H), 2.23 (s, 6H), 1.67 (m, 2H), 1.22 (d, *J* = 4 Hz, 6H).

4-Cyclopropyl-*N*¹-(3-(dimethylamino)propyl)-*N*¹-methylbenzene-1,2-diamine. Step 1. To a round-bottom flask at 0 °C were added 4-bromo-1-fluoro-2-nitrobenzene (10.0 g, 45.5 mmol) and *N,N,N'*-trimethylpropane-1,3-diamine (6.99 mL, 47.7 mmol). The reaction was allowed to warm to room temperature and stirred for 16 h. The reaction was extracted into EtOAc, washed once with saturated aqueous NaHCO₃ and twice with water, and then dried over Mg₂SO₄. The organic layer was filtered and concentrated to yield 11.1 g (77%) of *N*-(4-bromo-2-nitrophenyl)-*N,N,N'*-trimethylpropane-1,3-diamine as a bright orange solid: ¹H NMR (400 MHz, DMSO-*d*₆) δ 7.93 (d, *J* = 2.6 Hz, 1H), 7.64–7.61 (dd, *J* = 2.6, 9.2 Hz, 1H), 7.24–7.21 (d, *J* = 9.2 Hz, 1H), 3.21–3.17 (m, 2H), 2.72 (s, 3H), 2.26–2.22 (m, 2H), 2.14 (s, 6H), 1.69–1.62 (m, 2H).

Step 2. To a pressure vessel were added 2-cyclopropyl-4,4,5,5-tetramethyl-1,3,2-dioxaborolane (900 mg, 5.36 mmol), potassium phosphate (3.0 g, 14 mmol), and water (0.8 mL). After stirring at room temperature for 15 min, *N*-(4-bromo-2-nitrophenyl)-*N,N,N'*-trimethylpropane-1,3-diamine (1.30 g, 4.12 mmol), palladium acetate (92 mg, 0.41 mmol), tricyclohexylphosphine (231 mg 0.824 mmol), and toluene (21 mL) were added. The reaction was sealed and stirred at 80 °C for 19 h. The reaction was then cooled to room

temperature, diluted with EtOAc, extracted into water, washed once with brine, dried over Mg₂SO₄, filtered, and concentrated to yield 4-cyclopropyl-*N*-(3-(dimethylamino)propyl)-*N*-methyl-2-nitrobenzenamine as a dark red-brown oil. The material was used without further purification: MS, *m/z* (C₁₅H₂₃N₃O₂) calcd 277.36, found 278 (MH).

Step 3. 4-Cyclopropyl-*N*-(3-(dimethylamino)propyl)-*N*-methyl-2-nitrobenzenamine (600 mg, 2.16 mmol) was dissolved in MeOH (22 mL). Palladium (115 mg, 0.108 mmol, 10% w/w on carbon) was added, a balloon containing hydrogen was inserted, and the reaction was stirred at room temperature for 18 h. The solution was then filtered through a pad of Celite and concentrated. The crude mixture was then purified by Gilson reverse-phase HPLC to yield 710 mg (72%) of title compound as a viscous red-brown oil: ¹H NMR (400 MHz, DMSO-*d*₆) δ 6.78 (d, *J* = 8.0 Hz, 1H), 6.34 (d, *J* = 2.0 Hz, 1H), 6.26 (dd, *J* = 2.0, 8.0 Hz, 1H), 4.79 (br s, 2H), 2.71 (m, 2H), 2.48 (s, 3H), 2.22 (m, 2H), 2.08 (s, 6H), 1.71 (m, 1H), 1.54 (m, 2H), 0.82 (m, 2H), 0.51 (m, 2H).

Solubility Determination. Aqueous solubility was determined according to an automated procedure.³³

Plasma Protein Binding. Plasma protein binding was determined by ultrafiltration according to an established procedure: 1 mM control and test compound solutions were prepared from 10 mM stock solutions (all in DMSO) by Biomek FX (check 10 mM stock solution for signs of precipitation/crystallization before use). If the 1 mM spiking solutions have been prepared and kept in the refrigerator overnight, thaw in room temperature, centrifuge the solutions at 3100 rpm for 3 min, and vortex at moderate speed for 1 min. Check for signs of precipitation/crystallization (with the aid of background lighting). Keep the spiking solutions at room temperature until use. Dispense 999 μL of 0.45 μm-filtered plasma into a 96-deep-well plate (according to predetermined plate map) for warm samples by hand. Add 1.0 μL of the 10 mM DMSO stock into each of the appropriate wells and mix by Biomek FX. Cover with a 96-well plate film and preincubate the warm samples at 37 °C for 45 min. Create cold samples by dispensing 99 μL of plasma ultrafiltrate into 96-shallow-well plate (according to predetermined plate map) by hand. Add 1.0 μL of the 1 mM DMSO stock solutions and 100 μL of quench solution [0.1% formic acid in can-H₂O (25:75) with 500 ng/mL internal standard] into each of the appropriate wells and mix by Biomek FX (cold samples are ready for LC–MS analysis). After preincubation of warm samples is done, aliquot 400 μL of each (in duplicate) into a Millipore Multiscreen filter plate by hand. Centrifuge the warm samples at 3000 rpm for 45 min at 37 °C. Aliquot 30 μL of ultrafiltrate (free fraction) from warm samples into a 96-well shallow plate. Add 30 μL of quench solution to warm samples and vortex (warm samples are ready for LC–MS analysis; mass spectrometry with Applied Biosystems API 3000 on Analyst 1.4.1 with Automaton).

Homogeneous Time-Resolved Fluorescence Enzyme Assays. IC₅₀'s for the inhibition of the Tie-2 kinase enzyme for individual compounds were measured using an HTRF assay, utilizing the following procedure: in a 96-well plate (available from Costar Co.) was placed 1 μL of each test and standard compound per well in 100% DMSO having a 25 μM final compound concentration (3-fold, 10 point dilution). To each well was added 20 μL of a reaction mix formed from Tie-2 (4.0 μL; of a 10 mM stock solution available from Gibco), 0.05% BSA (0.1 μL; from a 10% stock solution available from Sigma-Aldrich Co.), 0.002 mM of BLC HER-2 KKK (Biotinylated Long chain peptide; 0.04 μL; from a 0.002 mM stock solution), 0.01 mM ATP (0.02 μL; commercially available from Sigma-Aldrich Co.), and water (15.84 μL) to bring the total volume to 20 μL/well.

The reaction was initiated in each well by adding 20 μL per well of an enzyme preparation consisting of a 50 mM concentration of HEPES (1.0 μL; from a 1000 mM stock solution commercially available from Gibco Co.), 0.05% BSA (0.1 μL), 4 mM DTT (0.08 μL; from a 1000 mM stock solution available from Sigma-Aldrich Co.), a 2.4 × 10⁻⁷ M Tie-2 (0.02 μL, from a 4 mM concentration stock), and the remaining volume being water (18.8 μL) to dilute the enzyme preparation to a total volume of 20 μL. The plate was

incubated for about 90 min at room temperature. After incubation, 160 μL of a filtered detection mixture [prepared from 0.001 mg/mL of SA-APC (0.0765 μL ; available as a 2.09 mg/mL stock solution from Gibco), 0.03125 nM Eu-Ab (0.1597 μL ; available in a 31.3 nM stock solution from Gibco), and water to bring the volume to 160 μL (159.73 μL)] was added to each well to stop the reaction therein. The plate was then allowed to equilibrate for about 3 h and read on a Ruby Star fluorescent reader (available from BMG Technologies, Inc.) using a four-parameter fit using activity base to calculate the corresponding IC_{50} 's for the test and standard compounds in each well.

IC_{50} 's for the inhibition of the KDR kinase enzyme for individual compounds were measured using an HTRF assay, utilizing the procedure described above for the Tie-2 kinase enzyme with the following changes: 1 μM gastrin (biotin long chain, EEEEAYGWLDF), 1 μM ATP, 50 pM His-tagged bisphosphorylated KDR kinase domain, 90 min reaction, 30 min after quench equilibrium; buffers, 50 mM HEPES pH 7.5, 50 mM NaCl, 10 mM MgCl_2 , 5 mM MnCl_2 , 0.05% BSA, 2 mM DTT.

Conditions for All Other Enzyme Assays. Peptide substrate sequences (all substrates at 1 μM unless stated otherwise) were as follows: gastrin, biotin (long chain) EEEEAYGWLDF free acid; HS-1B, biotin (long chain) EQEDEPEGIYGVLF free acid; HER-2, biotin (long chain) GGMEDIYFEFMGGKKK free acid; ATF2, biotinylated natural protein substrate, kinase dead, N-term Avitag; PLK, biotin (long chain) AGAGRRRSLELHKR free acid; CDK1, biotin (long chain) VIPINGSRPTPRRGQNR free acid; GFAP, biotin (long chain) RRRITSAARRS free acid; poly EY, from Sigma (P7244), poly(Glu, Tyr) sodium salt (4:1). The following are the peptides/enzyme constructs used: PDGF-poly EY/GST KD, TrkA-gastrin/GST KD, EpHB4-HS-1B/GST KD, cFMS-HER-2/GST KD, Lck-gastrin/GST KD, Src-gastrin/GST KD, Lyn-gastrin/GST FL, Fgr-gastrin/GST KD, Fes-gastrin/GST KD, Btk-gastrin/GST KD, Syk-gastrin/His KD, Zap70-gastrin/His KD, EGFR-gastrin/GST KD, IGFR-1-gastrin/GST KD, Irk-gastrin/GST KD, cMet-gastrin/GST KD, Ret-gastrin/GST KD, Abl-HS-1B/GST KD, Jak3-HER-2/GST KD, Itk-HS-1B/GST KD, Csk-HS-1B/GST FL, p38a-ATF2 (100 nM)/His FL, JNK3-ATF2 (100 nM)/GST FL, CDK5-CDK1/(100 nM)/His FL, PKBa-GFAP (50 nM)/His FL, AuroraA-PLK/His KD (KD = kinase domain; FL = full length; GST = glutathione-S-transferase tagged; His = His tagged). All assays were quenched within the linearity of the enzyme. All assays were run at the K_m for ATP. Buffer conditions for all assays are based on the KDR example with minor variations on the same theme. PDGF was determined by a radioactive filtration assay. MAPH filter plates and 1 Ci/mmol ^{32}P were used.

Cell-Based Tie-2 Autophosphorylation Assay. The IC_{50} of the test compounds for inhibition of Tie-2 autophosphorylation was determined using a plate-based immunoassay using the Delfia detection platform. EA.hy926 cells were cultured in a growth medium solution containing DMEM supplemented with 10% FBS serum and penicillin-streptomycin-glutamine. The cells were plated in 24-well tissue culture plates at a final cell density of 2×10^5 cells/well. The cells were incubated for 5 h at 37 $^\circ\text{C}$. Medium was then removed, and the cells were washed twice with 500 μL of PBS at room temperature. A 500- μL portion of F12 nutrient mixture supplemented with 0.5% FBS was then added to each well, and the cells were incubated at 37 $^\circ\text{C}$ overnight. Immediately prior to the addition of test compound, media was replaced with a preparation of 500 μL of DMEM plus 1% BSA.

Anti-hTie2 antibody (100 μg) (R & D Systems, Inc., AF313) was diluted with 10 mL of ice-cold PBS to prepare a 10 $\mu\text{g}/\text{mL}$ antibody concentration stock. A 96-well microplate (Perkin-Elmer Wallac, AAAND-0001) was coated with 100 μL of the anti-Tie-2 antibody stock and the plate was stored at 4 $^\circ\text{C}$ overnight. The plates were washed three times with 200 μL of PBS 0.1% Tween20 and blocked for 1 h by 5% BSA. The plates were then stored at room temperature for about 1 h.

A 20- μL aliquot of a selected Tie-2 reference compound was placed in a selected well of a 96-well plate, diluted 1:4 with 100%

DMSO from an initial concentration of 10 mM to a final concentration of 2.5 mM, and then diluted 1:3 with 100% DMSO for a 10-point dilution to a final concentration of 0.128 μM . Test compounds (10 μL of a 10 mM concentration) were similarly diluted 1:4 with 100% DMSO to obtain a sample concentration of 2.5 mM and then diluted 1:3 for a 10-point dilution to finally obtain a concentration of 0.128 μM for each test compound. DMSO (20 μL) served as a positive control, and 10 μL of the 2.5 mM reference compound served as the negative control. A 2- μL aliquot from each well (test compounds and positive and negative controls) in the 96-well plate was added to designated wells in the 24-well cell culture plate (1:250 dilution). The culture plate was incubated for 2.5 h at 37 $^\circ\text{C}$. Tie-2 autophosphorylation was then stimulated by the addition of angiotensin-1. Recombinant human Ang1 was diluted to final concentration of 10 $\mu\text{g}/\text{mL}$ in 1% BSA/DMEM and stored on ice. hAng1 (5 μL of 10 $\mu\text{g}/\text{mL}$ solution) was added to each well of the 24-well plate containing the EA.hy926 cells. The plate was then shaken at 700 rpm at 37 $^\circ\text{C}$ for about 2.5 min. After shaking, the wells were incubated for a further 7.5 min at 37 $^\circ\text{C}$. The medium was removed and 400 μL of ice-cold PBS + 300 μM NaVO_4 was added. The wells were kept on ice for at least 5 min and washed one time with ice-cold PBS containing 300 μM NaVO_4 . The cells were lysed with 150 μL of RIPA, containing 300 μM NaVO_4 and a protease inhibitor cocktail (Sigma-Aldrich, P8340). The cells were lysed on ice for 30 min.

Cell lysate (140 μL) was added to the antibody-coated plate and the plate was incubated at 4 $^\circ\text{C}$ for 2 h. The lysate was removed and the plate was washed three times each with 400 μL of Delfia wash buffer. The plate was tap-dried with a paper towel. The anti-phosphotyrosine antibody 4G10 (Upstate, 05-321) was diluted with Delfia assay buffer to make a solution of about 1 $\mu\text{g}/\text{mL}$. Diluted antibody (100 μL) was added to the plate and the plate was incubated at room temperature for 1 h. The plate was again washed three times with 400 μL of wash buffer. Eu-N1-labeled anti-mouse antibody (Perkin-Elmer Wallac, AD0124) was diluted with Delfia assay buffer to a final concentration of 0.1 $\mu\text{g}/\text{mL}$. Diluted antibody (100 μL) was added to each well of the plate, and the plate was incubated at room temperature for 1 h. The plate was washed three times as described above. Delfia enhancement solution (100 μL , Perkin-Elmer Wallac, 1244-105) was added to each well and the plate was incubated at room temperature for 5 min in the dark. The europium signal was measured with a Victor multilabel counter (Wallac Model 1420). Raw data were analyzed using a fit equation in XLFit. IC_{50} values were then determined using Grafit software.

Tie-2 Pharmacodynamic Assay. The effect of **63** on Tie-2 phosphorylation was evaluated in the lungs of female CD-1 NU/NU mice ($N = 3/\text{group}$). **63** was administered by oral gavage at 100 mg/kg at the zero hour time point. Tie-2 phosphorylation was induced by recombinant human Angiotensin-1 (R&D Systems Inc., Minneapolis, MN). Angiotensin-1 (12 μg) was administered intravenously 15 min prior to the 3, 8, and 12 h time points. Then the lungs were immediately dissected and snap frozen in liquid nitrogen. Blood samples were taken by cardiac puncture to determine compound concentrations in the plasma.

Individual mouse lungs were homogenized in 0.75 mL of RIPA buffer containing 300 μM NaVO_4 and a protease inhibitor cocktail (Sigma-Aldrich, P8340). The insoluble debris was removed following centrifugation at 4 $^\circ\text{C}$ for 15 min at 14 000 rpm. The supernatants were then precleared with 50 μL of protein A/G agarose beads (Sigma) for 1 h at 4 $^\circ\text{C}$. The supernatants were then centrifuged at 3000 rpm for 2 min and the supernatants decanted into a fresh Eppendorf. The protein concentration of each lysate was determined using the colorimetric RC DC system (Bio-Rad, 500-0121) and the concentration adjusted to 10 mg/mL by dilution in complete RIPA lysis buffer.

Tie-2 was immunoprecipitated from 2 mg of total protein overnight at 4 $^\circ\text{C}$ by 4 μg anti-murine Tie-2 antibody (R&D, AF762) in the presence of 50 μL of protein A/G beads (Pierce, 20421). The protein A/G beads were recovered by centrifugation and washed four times in RIPA buffer containing 300 μM NaVO_4 and a protease inhibitor cocktail (Sigma-Aldrich, P8340). The beads

were resuspended in 50 μL of $2\times$ sample buffer and resolved on a 10% polyacrylamide gel under denaturing and reduced conditions. The proteins were then transferred to a nitrocellulose membrane. The membrane was then blocked overnight in blocking buffer (0.25% gelatin in TBST, 20 mM Tris-HCl pH 7.4, 150 mM NaCl, 0.1% Tween 20). The nitrocellulose filter was then probed with anti-phosphotyrosine 4G10 antibody at a concentration of 0.5 $\mu\text{g}/\text{mL}$ in blocking buffer for 2 h at room temperature. The filter was washed three times in blocking buffer and probed with horseradish peroxidase conjugated anti-mouse IgG (Amersham, NA931V, 1:3000 dilution) for 1 h. The filter was washed three times in blocking buffer. Phosphorylated Tie-2 was detected using a chemiluminescent method and quantified using a chemiluminescent imaging system (Bio-Rad). Images were recorded on Kodak scientific imaging film.

The filter was then stripped and the filter was then probed with the anti-murine Tie-2 antibody (R&D, AF762) for 2 h at room temperature. The blot was washed three times in wash buffer and incubated with horseradish peroxidase-linked anti-goat Ig (Dako-Cytomation, P0160, 1:3000 dilution) for 1 h at room temperature. The filter was washed three times in blocking buffer. Total Tie-2 was detected using a chemiluminescent method and quantified using a chemiluminescent imaging system (Bio-Rad). Images were recorded on Kodak scientific imaging film.

Pharmacokinetic Studies. Male Sprague–Dawley rats with surgically implanted femoral vein and jugular vein cannulae were obtained from Charles River Laboratories (Boston, MA). Animals were fasted overnight, and the following day compounds were administered either by oral gavage or by intravenous bolus injection ($N = 3$ animals per study). Oral formulations were made 24–48 h prior to dosing, while intravenous formulations were made on the day of dosing. Blood samples were collected over 24 h via jugular cannula into a heparinized tube. Following centrifugation, plasma samples were stored in a freezer to maintain $-70\text{ }^\circ\text{C}$ until analysis. Lithium-heparinized plasma samples (50 μL) were precipitated with 100% acetonitrile containing the internal standard (IS). The supernatant was transferred into a 96-well plate, and an aliquot of 20 μL was injected onto an LC–MS/MS system. The analytes were separated by a reversed-phase C-18 analytical column. The analyte ions were generated by an electrospray ionization (ESI) source and detected by a Sciex API3000 triple quadrupole mass spectrometer operated in the multiple reaction monitoring (MRM) mode. Study sample concentrations were determined from a weighted ($1/x^2$) linear regression of peak area ratios (analyte peak area/IS peak area) versus the theoretical concentrations of the calibration standards. Pharmacokinetic parameters were calculated using a small molecules discovery assay (SMDA) within the computer program Watson (InnaPhase).

Acknowledgment. We thank our colleagues Nick Paras for the synthesis of **43** and Helming Tan and Maggie Wacker for the 0.01 N HCl Symyx solubility assay.

Supporting Information Available: Elemental analysis, HPLC, X-ray crystallographic, and pharmacodynamic model data. This material is available free of charge via the Internet at <http://pubs.acs.org>.

References

- Risau, W. Mechanism of angiogenesis. *Nature* **1997**, *386*, 671–674.
- Walsh, D. A.; Haywood, L. Angiogenesis: A therapeutic target in arthritis. *Curr. Opin. Invest. Drugs* **2001**, *2*, 1054–1063.
- Detmar, M. The role of VEGF and thrombospondin in skin angiogenesis. *Dermatol. Sci.* **2000**, *24*, S78–S84.
- (a) Folkman, J. Anti-angiogenesis: New concept for therapy of solid tumors. *Ann. Surg.* **1972**, *175*, 409–416. (b) Folkman, J. Tumor angiogenesis: Therapeutic implications. *N. Engl. J. Med.* **1971**, *285*, 1182–1186.
- (a) Holmgren, L.; O'Reilly, M. S.; Folkman, J. Dormancy of micrometastases: Balanced proliferation and apoptosis in the presence of angiogenesis suppression. *Nat. Med.* **1995**, *1*, 149–153. (b) Folkman, J. What is the evidence that tumors are angiogenesis dependent? *J. Nat. Cancer Inst.* **1990**, *82*, 4–6.
- Shawver, L. K.; Lipson, K. E.; Fong, T. A. T.; McMahon, G.; Plowman, G. D.; Strawn, L. M. Receptor tyrosine kinases as targets for inhibition of angiogenesis. *Drug Discovery Today* **1997**, *2*, 50–63.
- Ferrara, N.; Gerber, H.-P.; LeCouter, J. The biology of VEGF and its receptors. *Nature Med.* **2003**, *9*, 669–676.
- (a) Fraley, M. E.; Hoffman, W. F.; Arrington, K. L.; Hungate, R. W.; Hartman, G. D.; McFall, R. C.; Coll, K. E.; Rickert, K.; Thomas, K. A.; McGaughey, G. B. Property-Based Design of KDR Kinase Inhibitors. *Curr. Med. Chem.* **2004**, *11*, 709–719. (b) Boyer, S. J. Small molecule inhibitors of KDR (VEGFR-2) kinase: An overview of structure activity relationships. *Curr. Top. Med. Chem.* **2002**, *2*, 973–1000.
- Manley, P. W.; Bold, G.; Brügggen, J.; Fendrich, G.; Furet, P.; Mestan, J.; Schnell, C.; Stolz, B.; Meyer, T.; Meyhack, B.; Stark, W.; Strauss, A.; Wood, J. Advances in the structural biology, design and clinical development of VEGF-R kinase inhibitors for the treatment of angiogenesis. *Biochim. Biophys. Acta* **2004**, 17–27.
- (a) Bold, G.; Altmann, K.-H.; Frei, J.; Lang, M.; Manley, P. W.; Traxler, P.; Wietfeld, B.; Brügggen, J.; Buchdunger, E.; Cozens, R.; Ferrari, S.; Furet, P.; Hofmann, F.; Martiny-Baron, G.; Mestan, J.; Rösel, J.; Sills, M.; Stover, D.; Acemoglu, F.; Boss, E.; Emmenegger, R.; Lässer, L.; Masso, E.; Roth, R.; Schlachter, C.; Vetterli, W.; Wyss, D.; Wood, J. M. New anilinothalazines as potent and orally well absorbed inhibitors of the VEGF receptor tyrosine kinases useful as antagonists of tumor-driven angiogenesis. *J. Med. Chem.* **2000**, *43*, 2310–2323.
- (a) Sun, L.; Liang, C.; Shirazian, S.; Zhou, Y.; Miller, T.; Cui, J.; Fukuda, J. Y.; Chu, J.-Y.; Nematalla, A.; Wang, X.; Chen, H.; Sista, A.; Luu, T. C.; Tang, F.; Wei, J.; Tang, C. Discovery of 5-[5-fluoro-2-oxo-1,2-dihydroindol-(3Z)-ylideneethyl]-2,4-dimethyl-1H-pyrrole-3-carboxylic acid (2-diethylaminoethyl)amide, a novel tyrosine kinase inhibitor targeting vascular endothelial and platelet-derived growth factor receptor tyrosine kinase. *J. Med. Chem.* **2003**, *46*, 1116–1119. (b) Fiedler, W.; Serve, H.; Döhner, H.; Schwittay, M.; Ottmann, O. G.; O'Farrell, A.-M.; Bello, C. L.; Allred, R.; Manning, W. C.; Chrrington, J. M.; Louie, S. G.; Hong, W.; Brega, N. M.; Massimini, G.; Scigalla, P.; Berdel, W. E.; Hossfeld, D. K. A phase 1 study of SU11248 in the treatment of patients with refractory or resistant acute myeloid leukemia (AML) or not amenable to conventional therapy for the disease. *Blood* **2005**, *105*, 986–993.
- (a) Bankston, D.; Dumas, J.; Natero, R.; Riedl, B.; Monahan, M.-K.; Sibley, R. A scaleable synthesis of BAY 43-9006: A potent Raf kinase inhibitor for the treatment of cancer. *Org. Proc. Res. Dev.* **2002**, *6*, 777–781. (b) Strumberg, D.; Richly, H.; Hilger, R. A.; Schleucher, N.; Korfee, S.; Tewes, M.; Faghii, M.; Brendel, E.; Voliotis, D.; Haase, C. G.; Schwartz, B.; Awada, A.; Voigtmann, R.; Scheulen, M. E.; Seeber, S. Phase I clinical and pharmacokinetic study of the novel Raf kinase and vascular endothelial growth factor receptor inhibitor BAY 43-9006 in patients with advanced refractory solid tumors. *J. Clin. Oncol.* **2005**, *5*, 965–972.
- (a) Mulcahy, M. F.; Benson, A. B., III. Bevacizumab in the treatment of colorectal cancer. *Expert Opin. Biol. Ther.* **2005**, *5*, 997–1005. (b) Hurwitz, H.; Ferenbacher, L.; Novotny, W.; Cartwright, T.; Hainsworth, J.; Heim, W.; Berlin, J.; Baron, A.; Griffing, S.; Holmgren, E.; Ferrara, N.; Fyfe, G.; Rogers, B.; Ross, R.; Kabbinavar, F. Bevacizumab plus irinotecan, fluorouracil, and leucovorin for metastatic colorectal cancer. *N. Engl. J. Med.* **2004**, *350*, 2335–2342. (c) Yang, J. C.; Haworth, L.; Sherry, R. M.; Hwu, P.; Schwartzentruber, D. J.; Topalian, S. L.; Steinberg, S. M.; Chen, H. X.; Rosenbert, S. A. A randomized trial of Bevacizumab, an anti-vascular endothelial growth factor antibody, for metastatic renal cancer. *N. Engl. J. Med.* **2003**, *349*, 427–434.
- (a) Yu, Q. The dynamic roles of angiopoietins in tumor angiogenesis. *Future Medicine* **2005**, *1*, 475–484. (b) Visconti, R. P.; Richardson, C. D.; Sato, T. N. Orchestration of angiogenesis and arteriovenous contribution by angiopoietins and vascular endothelial growth factor (VEGF). *Proc. Natl. Acad. Sci. U.S.A.* **2002**, *99*, 8219–8224.
- (a) Cho, C.-H.; Kammerer, R. A.; Lee, H. J.; Steinmetz, M. O.; Ryu, Y. S.; Lee, S. H.; Yasunaga, K.; Kim, K.-T.; Kim, I.; Choi, H.-H.; Kim, W.; Kim, S. H.; Park, S. K.; Lee, G. M.; Koh, G. Y. COMP-Ang1: A designed angiopoietin-1 variant with nonleaky angiogenic activity. *Proc. Natl. Acad. Sci. U.S.A.* **2004**, *101*, 5547–5552. (b) Suri, C.; Jones, P. F.; Patan, S.; Bartunkova, S.; Masionpierre, P. C.; Davis, S.; Sato, T. N.; Yancopoulos, G. D. Requisite role of angiopoietin-1, a ligand of the TIE2 receptor, during embryonic angiogenesis. *Cell* **1996**, *87*, 1171–1180.
- (a) Scharpfenecker, M.; Fiedler, U.; Reiss, Y.; Augustin, H. G. The Tie-2 ligand angiopoietin-2 destabilizes quiescent endothelium through an internal autocrine loop mechanism. *J. Cell Science* **2005**, *118*, 771–780. (b) Lobov, I. B.; Brooks, P. C.; Lang, R. A. Angiopoietin-2 displays VEGF-dependent modulation of capillary structure and endothelial cell survival in vivo. *Proc. Natl. Acad. Sci.*

- U.S.A. **2002**, 99, 11205–11210. (c) Oliner, J.; Min, H.; Leal, J.; Yu, D.; Rao, S.; You, E.; Tang, X.; Kim, H.; Meyer, S.; Han, S. J.; Hawkins, N.; Rosenfeld, R.; Davy, E.; Graham, K.; Jacobsen, F.; Stevenson, S.; Ho, J.; Chen, Q.; Hartmann, T.; Michaels, M.; Kelley, M.; Li, L.; Sitney, K.; Martin, F.; Sun, J.-R.; Zhang, N.; Lu, J.; Estrada, J.; Kumar, R.; Coxon, A.; Kaufman, S.; Pretorius, J.; Scully, S.; Cattle, R.; Payton, M.; Coats, S.; Nguyen, L.; Desilva, B.; Ndifor, A.; Hayward, I.; Radinsky, R.; Boone, T.; Kendall, R. Suppression of angiogenesis and tumor growth by selective inhibition of angiopoietin-2. *Cancer Cell* **2004**, 6, 507–516.
- (17) For an example from Abbott Laboratories, see: (a) Bump, N. J.; Arnold, L. D.; Dixon, R. W.; Höeffken, H. W.; Allen, K.; Bellamacina, C. (BASF) Method of identifying inhibitors of receptor tyrosine kinase Tie-2 for regulation of neovascularization. WO 01072778, 2001. (b) Arnold, L. D. Molecular interactions of potent angiogenesis inhibitors bound to Tie-2. In *Pre-Clinical Development, Protein Kinases in Drug Discovery and Development Conference*, Newark, NJ, Oct 15–16, 2001. For an example by GlaxoSmithKline, see: (c) Kaspavec, J.; Johnson, N. W.; Yuan, C.; Murray, J. H.; Adams, J. L. *Abstracts of Papers*, 229th National Meeting of the American Chemical Society, San Diego, CA, March 13–17, 2005; American Chemical Society: Washington, DC, 2005; MEDI 134.
- (18) Compounds were first described: Geuns-Meyer, S. D.; Hodous, B. L.; Chaffee, S. C.; Tempest, P. A.; Olivieri, P. R.; Johnson, R. E.; Albrecht, B. K.; Patel, V. F.; Cee, V. J.; Kim, J. L.; Bellon, S.; Zhu, X.; Cheng, Y.; Xi, N.; Romero, K.; Nguyen, H. N.; Deak, H. L. (Amgen, Inc.) Preparation of nitrogen-heteroaryl-containing protein kinase modulators for use against cancer and other diseases. WO 05113494, 2005.
- (19) Kuo, D. L. Magnesium chloride catalysed acylation reaction. *Tetrahedron* **1992**, 48, 9233–9236.
- (20) Geuns-Meyer, S. D.; DiPietro, L. V.; Kim, J. L.; Patel, V. F. (Amgen, Inc.) Triazinyl amide derivatives as angiogenesis inhibitors. WO 02083654, 2002.
- (21) (a) Singh, H.; Singh, A. K.; Sharma, S.; Iyer, R. N.; Srivastava, O. P. Synthesis of 5-chloro-3'-nitro-4'-substituted salicylanilides, a new series of anthelmintic and antimicrobial agents. *J. Med. Chem.* **1977**, 20, 826–829. (b) Kohrt, J. T.; Filipki, K. J.; Rapundalo, S. T.; Cody, W. L.; Edmunds, J. J. *Tetrahedron Lett.* **2000**, 41, 6041–6044.
- (22) (a) Miyaura, N.; Yanagi, T.; Suzuki, A. The palladium-catalyzed cross-coupling reaction of phenylboronic acid with haloarenes in the presence of bases. *Synth. Commun.* **1981**, 11, 513–519. (b) Watanabe, T.; Miyaura, N.; Suzuki, A. Synthesis of sterically hindered biaryls via the palladium-catalyzed cross-coupling reaction of arylboronic acids or their esters with haloarenes. *Synlett* **1992**, 207–210.
- (23) In general, trialkylphosphines are not thought to be particularly effective under aqueous conditions because they are prone to oxidation. For a general review on palladium-catalyzed coupling reactions of aryl chlorides and trialkyl phosphine ligands see: Littke, A. F.; Fu, G. C. Palladium-catalyzed coupling reactions of aryl chlorides. *Angew. Chem. Int. Ed.* **2002**, 41, 4176–4211.
- (24) (a) Askew, B.; Adams, J.; Booker, S.; Chen, G.; DiPietro, L. V.; Elbaum, D.; Germain, J.; Geuns-Meyer, S. D.; Habgood, G. J.; Handley, M.; Huang, Q.; Kim, T.-S.; Li, A.; Nishimura, N.; Nomak, R.; Patel, V. F.; Riahi, B.; Kim, J. L.; Xi, N.; Yang, K.; Yuan, C. C. (Amgen, Inc.) Preparation of 2-aminopyridine-3-carboxamides as remedies for angiogenesis mediated diseases. WO 03225106, 2003. (b) Manley, P. W.; Furet, P.; Bold, G.; Brügggen, J.; Mestan, J.; Meyer, T.; Schnell, C. R.; Wood, J.; Haberey, M.; Huth, A.; Kruger, M.; Menrad, A.; Ottow, E.; Seidelmann, D.; Siemeister, G.; Thierauch, K. H. Anthranilic acid amides: A novel class of antiangiogenic VEGF receptor kinase inhibitors. *J. Med. Chem.* **2002**, 45, 5687–5693.
- (25) (a) Martin, A. *Physical Pharmacy*, 4th ed.; Lippincott, Williams and Wilkins: New York, 1993; pp 212–250, and references therein. (b) Wan, X. Influence of the intramolecular hydrogen bonds on the properties of compounds. *Daxue Huaxue* **1994**, 9, 58–62.
- (26) Bridges, A. J. Chemical inhibitors of protein kinases. *Chem. Rev.* **2001**, 101, 2541–2571.
- (27) Shewchuk, L. M.; Hassell, A. M.; Ellis, B.; Holmes, W. D.; Davis, R.; Horne, E. L.; Kadwell, S. H.; McKee, D. D.; Moore, J. T. Structure of the Tie2 RTK domain: Self-inhibition by the nucleotide binding loop, activation loop, and C-terminal tail. *Structure* **2000**, 8, 1105–1113. For X-ray analysis of the extracellular Tie-2 receptor and Ang-2, see: Barton, W. A.; Tzvetkova-Robev, D.; Miranda, E. P.; Kolev, M. V.; Rajashankar, K. R.; Himanen, J. P.; Nikolov, D. B. Crystal structures of the Tie2 receptor ectodomain and the angiopoietin-2–Tie2 complex. *Nat. Struct. Mol. Biol.* **2006**, 13, 524–532.
- (28) For references comparing DFG-in and DFG-out binding, see: (a) Nagar, B.; Bornmann, W. G.; Pellicena, P.; Schindler, T.; Veach, D. R.; Miller, W. T.; Clarkson, B.; Kuriyan, J. Crystal structures of the kinase domain of c-Abl in complex with the small molecule inhibitors PD173955 and imatinib (STI-571). *Cancer Res.* **2002**, 62, 4236–4243. (b) Tokarski, J. S.; Newitt, J. A.; Chang, C. Y. J.; Cheng, J. D.; Wittekind, M.; Kiefer, S. E.; Kish, K.; Lee, F. Y. F.; Borzilleri, R.; Lombardo, L. J.; Xie, D.; Zhang, Y.; Klei, H. E. The structure of Dasatinib (BMS-354825) bound to activated ABL kinase domain elucidates its inhibitory activity against Imatinib-resistant ABL mutants. *Cancer Res.* **2006**, 66, 5790–5797. For general references on kinase X-ray structures, see: (c) Cherry, M.; Williams, D. H. Recent kinase and kinase inhibitor X-ray structures: Mechanisms of inhibition and selectivity insights. *Curr. Med. Chem.* **2004**, 11, 663–673. (d) Fischer, P. M. The design of drug candidate molecules as selective inhibitors of therapeutically relevant protein kinases. *Curr. Med. Chem.* **2004**, 11, 1563–1583. (e) Liu, Y.; Gray, N. S. Rational design of inhibitors that bind to inactive kinase conformations. *Nat. Chem. Biol.* **2006**, 2, 358–364.
- (29) For a reference discussing “non-traditional” hydrogen bonding, see: Pierce, A. C.; Sandretto, K. L.; Bemis, G. W. Kinase inhibitors and the case for CH \cdots O hydrogen bonds in protein-ligand binding. *Proteins: Struct., Funct., Genet.* **2002**, 49, 567–576.
- (30) (a) Lipinski, C. A.; Lombardo, F.; Dominy, B. W.; Feeney, P. J. Experimental and computational approaches to estimate solubility and permeability in drug discovery and development settings. *Adv. Drug Delivery Rev.* **1997**, 23, 3–25. (b) Veber, D. F.; Johnson, S. R.; Cheng, H.-Y.; Smith, B. R.; Ward, W. K.; Kopple, K. D. Molecular properties that influence the oral bioavailability of drug candidates. *J. Med. Chem.* **2002**, 45, 2615–2623.
- (31) Ali, M. H.; Buchwald, S. L. An improved method for the palladium-catalyzed amination of aryl iodides. *J. Org. Chem.* **2001**, 66, 2560–2565.
- (32) Mann, J.; Shervington, L. A. Synthesis of novel N- and S-mustards as potential prodrugs activated by bioreductive processes. *J. Chem. Soc., Perkin Trans. 1: Org. Bio-Org. Chem. (1972–1999)* **1991**, 12, 2961–2964.
- (33) Tan, H.; Semin, D.; Wacker, M.; Cheetham, J. An automated screening assay for determination of aqueous equilibrium solubility enabling SPR study during drug lead optimization. *J. Assoc. Lab Automat.* **2005**, 364–373.

JM061107L